Assimilation of GOES Infrared Brightness Temperatures with an Ensemble Kalman Filter: Track and Intensity Impacts for Hurricane Rita (2005)

By

Lisha M. Roubert

A thesis submitted in partial fulfillment of
the requirements for the degree of

Master of Science
(Atmospheric and Oceanic Sciences)

At the

UNIVERSITY OF WISCONSIN-MADISON

2012

Abstract

Data assimilation using ensemble Kalman filters (EnKF) has led to significant improvements in atmospheric state estimation. The advantages of EnKF over common operational assimilation methods such as three-dimensional variational (3D-VAR) methods and its impressive performance in the assimilation of radar data at convective scales have led to its increasing popularity. While most previous studies have involved the assimilation of conventional observations only, this study presents an innovative approach in the EnKF assimilation scheme that involves the assimilation of GOES -12 channel 3 (6.5 micron) and channel 4 (i.e. 10.7 micron) brightness temperature data. In this study, the potential of the assimilation of GOES-12 infrared brightness temperature data was explored in the context of track and intensity forecasts for hurricane Rita from the 2005 Atlantic hurricane season.

The experiments were run at two different resolutions. In the lower resolution experiments (60 km horizontal grid spacing) results show that the assimilation of GOES brightness temperatures improved the representation of TC structure and produced better track and intensity forecasts when compared to the control experiment (CTL), which involved conventional observations only. RMS errors and calibration values of different fields produced by the assimilation of GOES-12 brightness temperatures generally compared well to the CTL results and in certain cases performed better than the CTL. An example of this is the microphysical fields, where the marked improvements shown by the assimilation of GOES radiance data is due to the close relationship between radiance and microphysics. It is also shown that the assimilation of radiance data eliminated a spurious cyclone that

developed in the CTL experiment, which further highlights the potential of geostationary radiance data assimilation. In the higher resolution experiments (18km horizontal grid spacing), the improvement was much more limited. However, RMS errors for certain fields indicated that the scheme certainly shows potential for future application in TC analysis and forecasting.

Acknowledgements

First and foremost, I would like to thank my research advisor, Will Lewis. Thank you for your patience and for taking time off your busy schedule to help me. Without your help this work would not have been possible as this project was very daunting and challenging, especially during the first few months. I would also like to thank Greg Tripoli for allowing me to work in his research group even though my background was in Mathematics. Thank you for your positive encouragement and for supporting my stay in the graduate school when things weren't going too well and I wasn't sure about staying. I also appreciate your critique on my work, even though it can be a bit harsh at times, as this helps me become a better researcher.

Thank you also to my committee, Will Lewis, Greg Tripoli, Steve Ackerman, and John Martin for taking time off their busy schedule to read this thesis. I appreciate your input to help make this work better.

I also would like to acknowledge the funding sources that made this project possible. The first year of this project was funded by the University of Wisconsin-Madison Advanced Opportunity Fellowship (AOF). Also, to Professor Steve Ackerman, thank you for funding me as a TA and PA. Without that I do not think it would have been possible for me to continue in this program. I have really enjoyed working with you, Bob, and Ralph and look forward to our continued collaboration during the next year as I transition to my new job at SSEC.

Finally, I would like to dedicate this work to my mother, Carmen. You are the most amazing parent in the world. Thanks for all the support you have provided me during my academic career. Most importantly, thank you for believing in me even when I didn't believe in myself.

Table of Contents

Chapter 1

Introduction

Tropical cyclone (TC) forecasting remains one of the most challenging areas in the atmospheric sciences. Since Gray's studies of TC formation in 1968, tropical cyclone forecasting has seen a constant evolution of forecasting techniques. While TC track forecasting skill has steadily improved due to the advances in numerical modeling and observing capabilities, deterministic predictions of TC intensity still score poorly in mean absolute error (MAE) verification (DeMaria et al. 2005; DeMaria and Gross 2003). The National Hurricane Center (NHC) reports that the official 48-hr intensity forecast errors for the Atlantic basin have decreased only by 17 % during the past 15 years (Rogers, 2006). This is a large contrast to the 45 % decrease in track forecast errors. A dramatic example of the need for increased skill in TC intensity forecasts was seen in 2005, in the days preceding landfall by Hurricane Katrina. Due to the large threat that TCs present to civilization, the ability to accurately predict the full development of these systems many hours in advance is crucial and has been the goal that many hurricane researchers strive for.

While our knowledge of TCs has vastly increased since the initial TC studies, intensity forecasting still presents many challenges. The limited improvement in TC intensity forecast skill over the last fifteen years can be attributed to three main things: limited internal TC observations; a limited understanding of TC intensification processes; and a limited understanding of internal TC microphysics (Rogers, 2006).

Collecting an appropriate number of internal observations spanning the life cycle of a TC is essential to understanding its development (Rogers, 2006). While TC track is primarily determined by the surrounding environmental profile, rapid changes of storm intensity are driven by highly variable, small scale dynamics internal to the storm. These features are not resolved by coarse models, and are difficult to observe, both due to the high temporal variability, but also due to the distance from land-based assets, and the difficult conditions at the center of the storm (Houze, 2007). This lack of predictive ability leads to a reactive stance to changing TC dynamics, such as formation of secondary eyewalls, eyewall replacement cycles, and transition to sheared or unsheared environments. Hurricane Katrina demonstrated the necessity of being able to anticipate such events, and understand their implications on coastal development.

Linked to a lack of high resolution internal observations is our limited understanding of TC intensification processes (Rogers, 2006). These challenges in fully understanding the physical processes governing hurricane intensification makes it difficult to set up proper physical parameterizations in NWP models (Karyampudi et al. 1998; Houze et al. 2006). Therefore, numerous studies have focused on investigating the physical processes associated with TC intensification in order to improve model physics (Frank 1977; Frank and Ritchie 1999; Montgomery et al. 2006). Of all the factors that contribute to TC intensification, storm scale vortex internal dynamics, thermodynamics, and ocean surface fluxes seem to be the essential processes that need to be captured in numerical models (Li and Pu, 2008). Certain physical parameterization schemes that have been developed to better simulate these processes has greatly aided in improving forecasts of TC intensity.

TC intensity, however, does not solely depend on storm physics. Previous studies have shown that representation of cloud microphysics schemes in NWP models greatly influences TC internal structure (Wang, 2002; Li and Pu, 2008, Zhu & Zhang, 2006). Li and Pu (2008) found that the minimum sea level pressure (MSLP) of a TC can vary up to 29 hPa depending on the cloud microphysics scheme that is applied. Zhu and Zhang (2006) had also previously illustrated the sensitivity of TC intensity forecasts to different cloud microphysics schemes in the MM5 model with the case study of Hurricane Bonnie (1998). They found that the weakest storm was produced when all ice particles were removed from the cloud microphysical processes while the fastest developing storm was produced when all evaporation processes were removed. Therefore, in addition to the storm-scale physics, accurately modeled microphysics is also essential in TC intensity forecasting.

In addition to these three challenges, it has long been argued that model resolution would continue to limit improvements in TC intensity forecasting. However, the recently completed High-Resolution Hurricane test (HRH), a part of the Hurricane Intensity Improvement Project (HFIP), has demonstrated that higher model resolution doesn't necessarily lead to better intensity forecasts (Davis. et. al, 2010; Bernadet, L., 2010). This is not an isolated result-Li and Pu (2008) also showed that applying a 1-km grid resolution to forecast intensity only produced a limited improvement, and that resolution failed to reproduce the real intensity of the TC.

Although improving model physics and microphysics has significantly aided in improving forecasts of TC intensity, these approaches cannot overcome deficiencies in model initial conditions. Inaccurate TC representation at the initial time will significantly deteriorate

the forecast, and observations at these early stages are often lacking (Rogers, 2006). For this reason, we have had to rely on statistical based methods, such as ensemble forecasting, to account for the uncertainty in initial conditions when initializing model forecasts. The main advantage of ensemble based assimilation is that in addition to providing an ensemble of analyses, the ensemble spread provides information on the flow dependent uncertainty in the forecast. While ensemble forecasting is not entirely new, studies which have used an ensemble Kalman filter (EnKF) approach have been particularly successful. Successful uses of ensemble forecasting with an EnKF include the assimilation of radar data at convective scales (Synder & Zhang, 2003; Zhang et. al. 2004; Zhang, F., 2009) as well as the assimilation of TC data from Hurricane Katrina (R. D. Torn and Gregory J. Hakim, 2009). The latter was able to produce accurate TC position estimates for this storm, which as we know, would have been invaluable in 2005.

Although improvements have been made with the advent of ensemble forecasting, TC intensity forecasting still remains a problem due to the disadvantages that current data collection methods present. Airborne reconnaissance remains the gold standard, but is necessarily limited since it is not cost effective, is time consuming, and can't begin to cover the initial conditions of every TC that develops. Low-earth orbiting (LEO) satellites have limited swaths and, therefore, limited sampling that does not cover much of the region of TC genesis. Accurate TC intensity forecasting requires observations that sample the TC core and its environment early and continuously, which is not possible with either airborne reconnaissance or LEO satellite data sources. To have any hope of simulating intensity and

structure changes, we need to observe TCs with sufficient frequency, coverage and resolution to capture these processes.

In order to solve this issue, this study proposes the use of data from geostationary satellites for data assimilation with an EnKF. Geostationary platforms, as opposed to aircraft reconnaissance and LEO satellites, offer superior coverage in time and space due to the fact that geostationary orbits are synchronous with earths' motion, and stationary relative to the earth's surface. Geostationary platforms allow us to obtain continuous data in the region of TC development and thus capture much more detail in the tropical cyclone structure early in its evolution. Continuous observations over the TC core and its environment provide information of small scale features that are essential to TC intensification. In addition to this, continuous observations could also provide information on vortex hot towers, rainbands, and secondary eyewalls as these are also important for TC intensity changes (Guimond, 2005; Houze 2006). GOES data can aid in further understanding TC intensification processes and lead to significant improvement in TC forecasting skill.

In Chapter 2 of this thesis, the potential of using GOES-12 channel 4 brightness temperature data for assimilation with an EnKF is explored. The GOES-12 10.7micron brightness temperature data assimilation scheme is presented and the impact of employing this scheme is assessed with the case study of Hurricane Rita (2005). This study verifies the impact of the GOES brightness temperature assimilation scheme on hurricane track and intensity forecasts, hurricane structure representation, and representation of microphysical and non-microphysical fields.

Results from a 60 km low resolution run performed in this experiment showed that the GOES brightness temperature assimilation produces improved results over the control experiment, which involved conventional observations only. In most areas that were examined, results from the experiments involving the assimilation of GOES brightness temperatures surpassed those from the control run. The assimilation of GOES brightness temperatures significantly improved the TC track forecast and also produced an intensity forecast with less error than the control. In addition to this, RMS errors for most non-microphysical fields were also lower than those of the control experiment. Moreover, results showed that the assimilation of GOES-12 brightness temperatures with an EnKF shows promise in eliminating current issues with spurious cyclone genesis.

Chapter 3 of this thesis study presents a discussion on the methodology employed for the experiments in Chapter 2 and also introduces alternate methods that could improve upon the obtained results. The bogussing TC initialization method is presented as a solution to remedy issues with sparse observations. The concept of perturbing the TC vortex to create an ensemble of analyses is also presented. Details on these procedures and their advantages are discussed. In addition to this, an overview of the next series of experiments, which employ the procedures discussed in this chapter, is presented.

The multiple areas of success of the low resolution run from Chapter 2 encouraged a second run at a higher resolution of 18 km. In Chapter 4, an 18km resolution is employed for simulations of Tropical Cyclone Rita. As in Chapter 2, GOES-12 10.7micron brightness temperatures are assimilated with an EnKF to assess the impact of these observations in the

forecast of track and intensity, representation of TC structure, and representation of microphysical and non-microphysical fields. A few different changes were made to the methodology that was used in Chapter 2. First, a bogussing scheme was employed for TC initialization in this study. In addition to this, a separate experiment was performed with the assimilation of GOES-12 water vapor observations to determine if assimilating these observations presented any improvement over the use of GOES-12 brightness temperatures.

Results from the experiments performed in Chapter 4 show that assimilating GOES-12 brightness temperatures and water vapor observations produce little improvement in all examined fields over the experiments involving conventional observations only. Track and intensity forecasts for the experiment involving conventional observations only were superior to those produced with the use of GOES-12 brightness temperatures and water vapor observations. However, there were certain non-microphysical fields where experiments incorporating GOES-12 brightness temperatures and water vapor observations outperformed those involving conventional observations only.

In comparisons of the experiments incorporating brightness temperatures with experiments incorporating water vapor observations, assimilating GOES-12 water vapor observations produced overall improved results over assimilating GOES-12 brightness temperatures. Errors for the majority of the examined fields were lower when assimilating GOES-12 water vapor observations. Although the results from both these experiments fell below those of the control (involving conventional observations only), there is potential for improvement in the future.

The final chapter of this thesis study, Chapter 5, presents conclusions on all the efforts that were carried out in this study and also discusses future work.

References

Bernardet, L., L. Nance, S. Bao, B. Brown, L. Carson, T. Fowler, J. Halley Gotway, C. Harrop and J. Wolff, 2010: The HFIP High-Resolution Hurricane Forecast test: overview and results of track and intensity forecast verification, presented at 29th Conference on Hurricanes and Tropical Meteorology, AMS, Tucson, AZ, May 9-14.

Davis, C.,Wang, W., Dudhia, J., and R. Torn, 2010: Does Increased Horizontal Resolution Improve Hurricane Wind Forecasts? *Wea*. *Forecasting*, **25**, 1826–1841.

DeMaria, M, and J. M. Gross, 2003: Evolution of tropical cyclone forecast models. *Hurricane! Coping with Disaster*, R. Simpson, Ed., Amer. Geophys. Union, 103–126.

DeMaria, M., M. Mainelli, L. K. Shay, J. Knaff, and J. Kaplan, 2005: Further improvements to the Statistical Hurricane Intensity Forecasting Scheme (SHIPS). *Wea*. *Forecasting*, **20,** 531–543.

Frank, W. M., 1977: The Structure and Energetics of the Tropical Cyclone I. Storm Structure. *Mon*. *Wea*. *Rev*., **105**, 1119–1135.

Frank, W. M., 1977: The Structure and Energetics of the Tropical Cyclone II. Dynamics and Energetics. *Mon. Wea. Rev.*, **105**, 1136–1150.

Frank, W. M., and E. A. Ritchie, 1999: Effects of Environmental Flow upon Tropical Cyclone Structure. *Mon. Wea. Rev.*, **127**, 2044–2061.

Guimond, S. R., Heymsfield, G. M., and F. Joseph Turk, 2010: Multiscale observations of Hurricane Dennis (2005): the Effects of Hot Towers on Rapid Intensification. J. Atmos. Sci., **67**, 633–654

Houze, R. A., and Coauthors, 2006: The Hurricane Rainband and Intensity Change Experiment: Observations and Modeling of Hurricanes Katrina, Ophelia, and Rita. *Bull.Amer. Meteor. Soc.*, **87**, 1503–1521.

Karyampudi, V. M., Lai, G. S., and J. Manobianco, 1998: Impact of Initial Conditions, Rainfall Assimilation, and Cumulus Parameterization on Simulations of Hurricane Florence (1988). *Mon. Wea. Rev.*, **126**, 3077–3101

Li, X., and Z. Pu, 2008: Sensitivity of Numerical Simulation of Early Rapid Intensification of Hurricane Emily (2005) to Cloud Microphysical and Planetary Boundary Layer Parameterizations. *Mon. Wea. Rev.*, **136**, 4819–4838.

Montgomery, M. T., and R. Kallenbach, 1997: A theory for vortex Rossby-waves and its application to spiral bands and intensity changes in hurricanes. *Quart. J. Roy. Meteor. Soc.,* **123,** 435–465.

Rogers, R., and Coauthors, 2006: The Intensity Forecasting Experiment: A NOAA Multiyear Field Program for Improving Tropical Cyclone Intensity Forecasts. *Bull. Amer.Meteor. Soc.*, **87**, 1523–1537.

Snyder, C., and F. Zhang, 2003: Assimilation of Simulated Doppler Radar Observations with an Ensemble Kalman Filter. *Mon. Wea. Rev.*, **131,** 1663–1677.

Torn, R. D., and G. J. Hakim, 2009: Ensemble Data Assimilation Applied to RAINEX Observations of Hurricane Katrina (2005). *Mon. Wea. Rev.*, **137**, 2817–2829.

Wang, Y. 2002: An explicit simulation of tropical cyclones with a triply nested movable mesh primitive equation model—TCM3. Part II: Model refinements and sensitivity to cloud microphysics parameterization. *Mon. Wea. Rev.,* **130,** 3022–3036.

Zhang, F., Snyder, C., and J. Sun, 2004: Impacts of Initial Estimate and Observation Availability on Convective-Scale Data Assimilation with an Ensemble Kalman Filter.

Mon. *Wea*. *Rev*., **132**, 1238-1253

Zhang, F., Weng, Y., Sippel, J. A., Meng, Z., and C. H. Bishop, 2009: Cloud-Resolving Hurricane Initialization and Prediction through Assimilation of Doppler Radar Observations with an Ensemble Kalman Filter. *Mon*. *Wea*. *Rev*., **137**, 2105–2125.

Zhu, T., and D.-L. Zhang, 2006: Numerical simulation of hurricane Bonnie (1998). Part II: Sensitivity to varying cloud microphysical processes. J. Atmos. Sci., 63, 109-126.

Chapter 2

Improving Track and Intensity Forecasts for Hurricane Rita from GOES-12 10.7 micron Brightness Temperature Assimilation with an Ensemble Kalman Filter

2.1) Introduction

Uncertainties in tropical cyclone (TC) initialization are one of the fundamental reasons for the current lack of skill in tropical cyclone intensity forecasts (Rogers, 2006). Observations taken over the tropical cyclone vortex by airborne reconnaissance are only available for select storms, which makes it challenging to obtain an accurate representation of the tropical cyclone structure during the initial state. Efforts focusing on improving model resolution have not shown significant results (Bernadet, L, 2010; Davis et. al., 2010) and improving model microphysics has, so far, only aided in resolving certain vortex features (LI, X., and A. PU, 2009). Despite the improvements made in the model physics, errors in the intensity forecast still exist due to poor initialization. Thus, numerical weather prediction relies on data assimilation based methods that allow the integration of all available observations to generate a set of plausible initial conditions that are used to initialize the forecast.

Even though many variants of data assimilation have been explored throughout the years, the ensemble based data assimilation scheme has become more common due to the advantages it presents over operational based assimilation methods such as 3D-VAR and 4D-

VAR. The main advantage of ensemble based assimilation is that in addition to providing an ensemble of analyses it can provide information of the flow dependent uncertainty, which is captured by the ensemble spread. Results from previous studies have shown that the spread predicted by the EnKF analysis captures well the observed distribution of error about the initial analysis (Toth, 2001). Among the successful applications of the EnKF is the assimilation of radar data at the convective scales (Synder & Zhang, 2003; Zhang, F., 2009). The EnKF has also shown excellent performance in the assimilation of observations from Hurricane Katrina and produced accurate TC position estimates for this storm without the need of vortex bogussing and repositioning methods (R. D. Torn and Gregory J. Hakim, 2009).

However, while data assimilation schemes have greatly aided in improving TC forecasting skill, accurate prediction of TC intensity still remains a challenge. Accurate TC intensity forecasting requires observations that sample the TC core and its environment on the space-time scales of the convective phenomena that must be defined in the models initial state. This requires high frequency observations over the period of fluctuation of the dynamical entity simulated. Airborne reconnaissance remains the gold standard, but it is necessarily limited to short periods of storm penetration, which is insufficient to capture any but the shortest period fluctuations. Moreover, the cost of even these observations is prohibitive on the scale necessary to capture all possible genesis events. Low-earth orbiting satellites have limited swaths and cannot sample with the space-time frequency necessary to define the storm scale structure. Therefore, to have any hope of simulating intensity and

structure changes, TC's must be observed with sufficient frequency over space-time periods, coverage and resolution to capture these processes.

In order to solve this issue, this study proposes the use of Geostationary Operational Environmental Satellites (GOES) brightness temperature data for assimilation with an EnKF in order to improve TC track and intensity forecasting skill. The geosynchronous orbit of GOES is ideal for monitoring regions of tropical cyclone development. This allows for observations of exceptional temporal continuity and allows observation of greater detail in the TC structure. GOES's continuous observations of small scale features within the TC and its environment during intensification may also aid in further improving the understanding of hurricane intensification processes. While GOES radiance data has not been previously employed for TC data assimilation studies, it has proven to be successful in assimilation studies involving cloudy sky conditions. Koyama et al. (2006) showed that temperature and moisture-sensitive channels of the GOES infrared sounder are useful for data assimilation in clear sky conditions and also in the presence of optically thin to moderate high level clouds. Their results showed that that the use of infrared sounding observations in data assimilation could improve temperature and humidity profiles below optically thin-moderate ice clouds. Due to these promising results, the author (Koyama et. al.) encouraged the use of GOES data under all weather conditions. In contrast to Koyama et. al. (2006), the assimilation experiment described in this paper involves the use of GOES-12 imager observations rather than GOES sounder data. As opposed to the sounder, the GOES-12 imager provides larger spatial coverage that is necessary for accurate TC forecasting.

The objective of this paper is to prove that the continuous assimilation of GOES-12 10.7 micron brightness temperatures (T_B) improves the representation of the TC structure in the model initial conditions despite its ability to see only the upper cloud surface. At the current time, GOES represents the only consistent source of large spatial and temporal scale data consistent with the space-time scales that we hypothesize are critical to TC intensity predictions. It is expected that improved dynamic representation of these TC structure at the initial time will lead to improved forecasts and predictability of track and intensity.

Hurricane Rita represents an ideal test case for such hypothesis. This storm went through rapid intensification as it passed over the Gulf of Mexico, where it went from category 3 to category 5 in less than 36 hours. It was a storm that went through an eyewall replacement cycle and also showed concentric eyewall development. Rapid intensification and eye wall structure changes in TC's make it challenging to obtain an accurate forecast of intensity. Simulating such intensity and structure change can be achieved with the use of GOES-12 T_B data. Although this would be better investigated with the use of a higher resolution, this study employs a coarse resolution of 60 km to perform the experiments as this is a test study that explores the potential of the use of GOES-12 data for TC predictions. Successful results would eventually lead to further experiments that would be performed at a higher resolution.

With Hurricane Rita identified as a suitable case study, the subsequent sections of this paper discuss details on the implementation of the experiments performed in this study. The second gives a brief overview of the EnKF. The third section discusses important features of

the University of Wisconsin-Madison Non-Hydrostatic Modeling System (UW-NMS) while the fourth section discusses the model configuration, experiment design and details of the EnKF implementation. Results are discussed in the fourth section and conclusions and presented in the final section.

2.2) The Ensemble Kalman Filter (EnKF) Assimilation Algorithm

The Ensemble Kalman filter (EnKF) is a Monte Carlo approximation to the original Kalman Filter (Kalman and Bucy 1961; Gelb et al. 1974). It was introduced by Evensen (1994) and since then it has been applied in numerous studies in the geophysical sciences. The popularity gained by the EnKF is mainly due to its relative ease of implementation as it requires no derivation of a tangent linear operator or adjoint equations, and no integrations backward in time (Evensen, 2004). Moreover, it is computationally feasible and also compares well to other sophisticated data assimilation methods of interest to the meteorological community (e.g. 4D-VAR).

The implementation of the EnKF is very simple. Its implementation is discussed below with equations taken from Houtekamer at Mitchell (1998). The basic analysis equation for the EnKF at time t is:

$$\boldsymbol{\Psi^a} = \boldsymbol{\Psi^f} + \boldsymbol{K}\left(\boldsymbol{O} - \boldsymbol{H\Psi^f}\right) \qquad i = 1, \ldots, N \qquad (1)$$

where $\boldsymbol{\Psi^f}$ is a an m-dimensional column vector containing the model forecast, $\boldsymbol{O}$ is a p-dimensional column vector of observations that are assimilated. $\boldsymbol{H}$ is an operator that interpolates the true state (generated by the model) to the observed quantities ($\boldsymbol{O}$). $\boldsymbol{K}$ is the Kalman gain matrix. As pointed out by Lewis et. al., the Kalman gain "provides the means for converting the discrepancy between model and observation at a particular point into a smooth increment applied to rest of the model domain" (Lewis et. al, 2006). $\boldsymbol{K}$ is defined as:

$$\boldsymbol{K = P^f H^T [H P^f H^T + R]^{-1}} \qquad (2)$$

where $\boldsymbol{R}$ is the *p x p* observation-error covariance matrix, $\boldsymbol{P^f}$ is the *m x m* background-error covariance matrix of the model forecast ($\boldsymbol{\Psi^f}$).

In the EnKF, $\boldsymbol{P^f}$ is approximated using the sample covariance from an ensemble of model forecasts. However, the full matrix $\boldsymbol{P^f}$ does not need to be calculated and stored as it is very impractical. Instead, $\boldsymbol{P^f H^T}$ and $\boldsymbol{H P^f H^T}$ are estimated directly using the ensemble (Evensen 1994; Houtekamer and Mitchell 1998).

$$\boldsymbol{P^f H^T = \frac{1}{N-1} \sum_{i=1}^{N} \left(\Psi^f - \overline{\Psi^f}\right)\left[H\left(\Psi^f - \overline{\Psi^f}\right)\right]^T} \quad (3)$$

$$\boldsymbol{H P^f H^T = \frac{1}{N-1} \sum_{i=1}^{N} H\left(\Psi^f - \overline{\Psi^f}\right)\left[H\left(\Psi^f - \overline{\Psi^f}\right)\right]^T} \quad (4)$$

where,

$$\overline{\boldsymbol{\Psi^f}} = \frac{\mathbf{1}}{\boldsymbol{N}} \sum_{\boldsymbol{i=1}}^{\boldsymbol{N}} \boldsymbol{\Psi^f} \qquad (5)$$

and N is the number of ensemble members. The overbar shown on variables denotes the ensemble mean.

Application of the EnKF requires that an initial ensemble of model states be defined. These "model states" are created by perturbing a best-guess estimate of the initial state. After the ensemble of initial conditions is created, the NWP model is run once for each ensemble member. Observations are then assimilated into the different ensemble first-guess fields where equations (3) and (4) are used to calculate $\boldsymbol{P^f H^T}$ and $\boldsymbol{H P^f H^T}$. Afterwards, equation 2 is used to calculate the Kalman gain $\boldsymbol{K}$, and the analysis for each ensemble member is then calculated from equation (1). The result of this is an ensemble of analyses that are then integrated forward to the next observation time.

One of the significant advantages of the EnKF over other assimilation methods is that it provides information on the flow dependent uncertainty in the forecast. The flow dependent uncertainty of the forecast is provided by the covariance matrix $\boldsymbol{P^f}$, or ensemble spread, which serves as a measure of forecast accuracy. The ensemble spread is flow dependent due to the method that is employed to calculate $\boldsymbol{K}$. Since $\boldsymbol{K}$ is calculated from an ensemble of model states it can evolve with the nonlinear dynamics of the NWP (as opposed to the original Kalman filter, where the Kalman gain was propagated according to a linear model) (Lewis, 2006). The "flow dependent" error statistics are a very attractive feature of the EnKF. Although the EnKF is a statistical method, it also takes into account the evolution of

the flow and thus the error statistics are employed to determine the confidence that can be attributed to such a forecast. Methods that are purely stochastic (i.e. that do not take into account dynamics of the flow) would not have information on the state of the flow and therefore wouldn't be as useful for determining the forecast uncertainty. Now that a brief overview has been given on the EnKF the next section will proceed to discuss the model that was employed for this study.

2.3) The UW-Madison Non Hydrostatic Modeling System (UW-NMS)

The primary mission of ensemble forecasting is to generate a set of plausible solutions which encompass the true state of the atmosphere. While ensemble techniques help improve the ability to predict the forecast uncertainty or error distribution, the quality of the model and initial conditions will determine the accuracy of the predictions of the mean state of the atmosphere. The model error is related to the systematic errors of a forecast, which can accumulate to further degrade forecast skill. Therefore, a model that accurately represents the dynamics and physics of the atmosphere is essential to the success of ensemble forecasting.

The numerical model used in this study is University of Wisconsin Non-Hydrostatic Modeling System (UW-NMS) described in Tripoli (1992). The UW-NMS is a time split compressible non hydrostatic model employing a single moment explicit bulk microphysics predictions. It is used here to simulate the interaction between convection and mesoscale or synoptic- scale phenomena. It uses ice-liquid water potential temperature as the prognostic thermodynamic variable since it is conserved during all phase changes. Potential

temperature, temperature, and cloud water are the diagnostic variables. The model is phrased on an Arakawa 'C' grid.

Of particular interest to the author are the schemes the UW-NMS incorporates to effectively treat numerical accuracy issues and represent moist convective processes. Integral constraints emphasizing conservation of kinetic energy, entropy, vorticity, and enstrophy are incorporated into the model to simulate more realistic energy spectra (Sadourny, 1969). It has been shown that these constraints lead to a reduction in the systematic accumulation of truncation errors that produce anomalous bifurcations from the physical solutions (Tripoli, 1992).

In addition to treating accumulation of truncation error, the UW-NMS shows marked improvement over other models in the representation of cloud convective processes with the use of the Modified Emanuel Convective Parameterization (CP) Scheme. This CP scheme regards the subcloud-scale drafts, instead of the clouds themselves, as the fundamental entities of moist convective transport (Emanuel, 1991). Accounting for the effects of these drafts is essential for accurate TC forecasting since convective downdrafts provide a mean to stabilize the atmosphere and therefore can weaken convection within the TC eye wall. Furthermore, these convective downdrafts can also prevent spontaneous genesis of TC's over warm oceans (Emanuel, 1989). The Emanuel CP scheme also addresses the issue of accounting for the redistribution of water, such as net fallout of precipitation, by introducing closure parameters linked to the cloud microphysics and dynamical processes. Specification

of these parameters leads to a more accurate representation of the vertical profiles of net heating and moistening by cloud processes (Emanuel, 1991).

Equally important to note are the major improvements that the UW-NMS presents over other nonhydrostatic modeling systems, such as its computationally efficient non-Boussinesq framework that conserves energy during transformations between kinetic, turbulent, and thermal energy. This proves to be essential for accurate TC forecasting.

The following section discusses the methodology of this case study and also presents details on the configuration of the model for this study.

2.4) Methodology

The objective of this study is to explore the potential of the assimilation of GOES-12 brightness temperature data to improve hurricane track and intensity forecasts. The EnKF is used to assimilate conventional (RAOB, METAR, ACARS, etc.) and GOES-12 10.7 micron brightness temperatures (T_B) observations to improve track and intensity forecasts for Hurricane Rita. Two experiments were performed in this study, one experiment with conventional observations only (CTL) and a second experiment assimilating both conventional and GOES-12 channel 4 brightness temperatures (CH4). The differences between results from the experiments were then examined to determine how the assimilation of GOES brightness temperatures impacts the forecast. While many centers possess resources to perform data assimilation procedures, this study acknowledges computational resource

limitations associated with atmospheric data assimilation. Therefore, a small size ensemble size was applied.

The CTL and CH4 experiments were performed at two different resolutions. Initially, a coarse resolution of 60 km was applied. A full analysis of the TC track, intensity, structure representation, as well as representation of microphysical and non-microphysical fields was done with the results of the low resolution run as a sensitivity test. More importantly, results from the low resolution experiments were used to determine the forecast bias, which was then employed to perform bias correction on the higher resolution experiments.

Upon analysis of the results from the 60 km resolution run, the experiments were run at a higher resolution of 18 km. The analysis done with the results from the 60 km resolution run were replicated for the 18 km resolution run. However, now being able to resolve the TC core, representation of mesoscale features essential to TC development and intensification was examined in more detail.

a. Model Configuration

The UW-NMS was initialized on a domain employing 40, 140 and 80 grid points respectively in the vertical, zonal and meridional directions. The grid spacing was of 60-km in the horizontal directions and 250-m stretched to 700-m in the vertical direction. A time step of 60s was used to integrate the model forward. A single moment bulk microphysics scheme was employed for rain and snow, and two-moment microphysics for cloud ice (Tripoli, 1992). Graupel and aggregates were not predicted.

b. Observations

As mentioned previously, two experiments were performed in this study, one experiment with conventional observations only (CTL) and a second experiment assimilating both conventional and GOES channel 4 brightness temperatures (CH4). The CTL experiment incorporated METAR (SLP), Aircraft Communication Addressing and Reporting System (ACARS (u, v, T)), RAOB (u, v, T, T_d), and POES (retrieved T, T_d) data obtained from the meteorological assimilation data ingest system (MADIS); and Vortex Information (lat, lon of TC center) data obtained from the TC VITALS. Cloud drift winds (AMV (u, v)) from GOES-11 and GOES-12 are also employed. The errors used for the conventional data are the NCEP Global Data Assimilation System (GDAS) values.

The CH4 experiment incorporates the GOES-12 Channel 4 10.7 micron brightness temperature data (thinned to 120km), which was retrieved from the NOAA Comprehensive Large Array-data Stewardship System (CLASS). An observation error of 10K was used in this study.

c. Ensemble Initialization and generation of perturbations

The Ensemble was initialized from the GFS analysis at 00Z on SEP 19 by perturbing the stream function and computing corresponding u, v and T perturbations with the method described by MH (Mitchell and Houtekamer, 2002). A 32 member ensemble was

created around that analysis. The procedure for generating perturbations is documented in detail in MH02 but will be discussed briefly in this paper for completeness.

To begin assimilating data it is necessary to have a model state $\boldsymbol{\Psi_c^f}(t_0)$ that will represent the most accurate estimate of the true state of the atmosphere $\boldsymbol{\Psi_t}(t_0)$ (Mitchell and Houtekamer, 2002). The true state of the atmosphere is unknown. Therefore, to obtain the model state that best represents the true state of the atmosphere equation (7) from HM 98 (Houtekamer and Mitchell, 1998) can be used:

$$\boldsymbol{\Psi_c^f}(t_0) = \boldsymbol{\Psi_t}(t_0) + \ random\ field \quad (1)$$

where the random field represents a random perturbation field added to the true state. Even though the true perturbation value is unknown, a set of solutions $\boldsymbol{\Psi_t}(t_0) + \boldsymbol{\Psi'}$ can be generated to include the truth $\boldsymbol{\Psi_c^f}$ or an error distribution $\boldsymbol{\Psi'}$ that has the random perturbation field within the estimated distribution. That is, it should satisfy:

$$\boldsymbol{\Psi_c^f}(t_0) \ \in \ \boldsymbol{\Psi_t}(t_0) + \boldsymbol{\Psi'} \quad (2)$$

The random perturbation field consists of u, v and T perturbations at each model level and a p_s perturbation. To obtain perturbations that are quasi geostrophically balanced, these u, v, T, and p_s perturbations are derived from a random stream function perturbation that is generated as a realization of a multivariate probability distribution (Mitchell et. al, 2002). The method to generate these stream function perturbations is discussed in detail in MH02 (Mitchell and Houtekamer, 2002).

Upon adding the perturbation field to $\boldsymbol{\Psi_t}(t_0)$, a model state $\boldsymbol{\Psi_c^f}(t_0)$ is obtained. This model state serves as the central state for the pair of initial ensemble of first guess fields

(Mitchell and Houtekamer, 2002). To obtain a pair of N member ensembles of first guess fields at time t_0, two sets of random perturbations are added to $\boldsymbol{\Psi_c^f}(t_0)$ as in equation (8) of HM 98:

$$\boldsymbol{\Psi_{i,j}^f}(t_0) = \boldsymbol{\Psi_c^f}(t_0) + \boldsymbol{random\ field_{i+(j-1)N}} \quad (3)$$

where the spread in the ensemble will represent the uncertainty in $\boldsymbol{\Psi_c^f}(t_0)$.

Now that the generation of the ensemble has been discussed the assimilation procedure will be described. A 27 hour spin up was allowed before beginning the assimilation of observations. For both CTL and CH4, a 3-hourly cycle was employed, meaning 9 total assimilation cycles between 03Z September 20 and 03Z September 21. To ascertain the impact of GOES-12 channel 4 brightness temperatures, the difference between the ensemble mean solutions of CH4 and CTL were examined. Details on the procedure for the assimilation of GOES brightness temperatures are discussed in the following section.

d. Assimilation of GOES Brightness Temperatures

The procedure used to assimilate GOES T_B is the same procedure that was applied to assimilate all other observations. The model was integrated forward and the Community Radiative Transfer Model (CRTM) was then used to compute model-based estimates of the 10.7 micron brightness temperature observations.

Some additional schemes were incorporated in the implementation of the EnKF to improve imbalances introduced by the covariance localization in the assimilation results. One

of the schemes applied was the Ensemble Square Root Filter method (EnSRF) developed by WH (Whitaker and Hamill, 2002) since it has shown to produce improved numerical precision and stability over the standard Kalman filter algorithm. The EnSRF eliminates the sampling error associated with perturbed observations and thus produces an analysis ensemble with an ensemble mean error that is lower than the EnKF for the same ensemble size (Whitaker and Hamil, 2002). In addition to this, a covariance relaxation technique with alpha=0.2 was applied (Zhang et al., 2004). To further improve the efficiency of the EnKF and filter distant-dependent covariance estimates, the Gaspari-Cohn covariance localization (Gaspari and Cohn, 1999) was also applied (900-km conventional, 240-km satellite). This method involves reducing the magnitude of covariance estimates more as the distance from the observation is increased. In this study, only data points within the specified km from the observation point can affect the analysis.

2.5) Results and Discussion

Nine total assimilation cycles between 03Z SEP 20 and 03Z SEP 21 were performed to assess the impact of the assimilation of GOES brightness temperatures on the simulation of Rita's track, intensity and representation of TC structure. In addition to this, the performance of the CH4 experiment on the representation of non-microphysical and microphysical fields is examined by comparisons of the ensemble mean solutions of the CTL and CH4 experiments and root-mean-square (RMS) analysis error. Results from both 60 km and 18 km resolution runs are presented and discussed below.

a. Tropical Cyclone Track Forecasts

First, the track forecasts for the CTL and CH4 experiments are compared to the best track positions to determine how well each of the experiments performed in the forecast of Hurricane Rita's track. The results are shown in Figure 1.

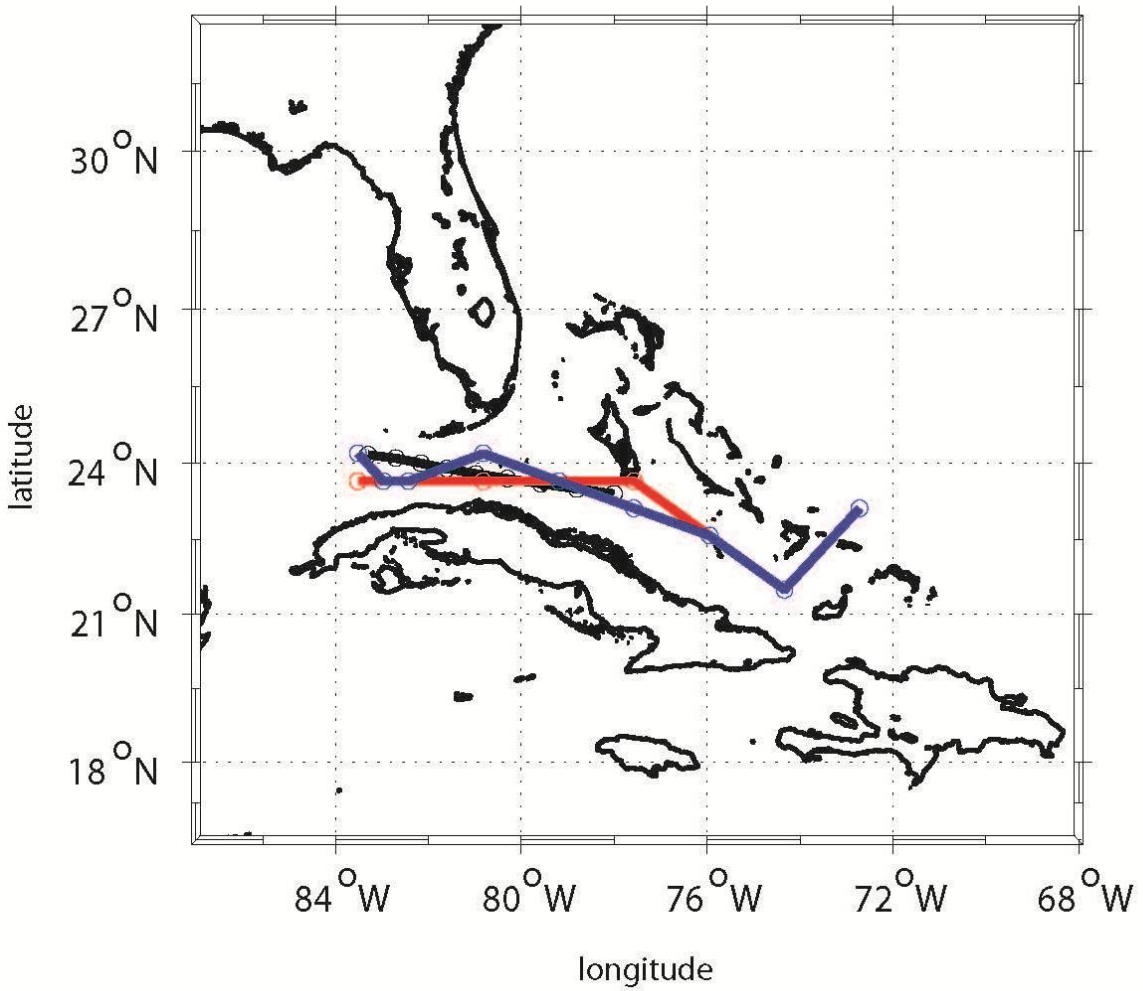

Figure 1. Track forecast for best track data in black, CTL experiment in red, and the CH4 experiment in blue. The data is plotted at every 3 hour intervals from September 20 03Z-September 21 03Z.

The best track data was originally available at 6 hour intervals from 0Z SEP 20 to 6Z SEP 21while the CTL and CH4 results were available at 3 hour intervals from 03Z SEP 20 to 03Z SEP 21. The best track data was interpolated with splines to obtain the corresponding values at 3 hour intervals so the results could then be compared to those obtained for the CTL and CH4 experiments. As shown in Figure 1, both the CTL and CH4 results compared well to the best track. However, the CH4 experiment performed significantly better than the CTL. Both experiments had similar initial values and remained similar for the first 3 times. After 12Z SEP 20, the track values for the CTL and CH4 gradually changed. Both remained close to the best track values throughout most of the simulation. However, at the final time the CH4 experiment results converged towards the same coordinates as the best track while the CTL results deviated further from the best track. Even with the large difference in the initial values between the best track and the two experiments, the final CH4 simulation results matched the best track. The CTL experiment, on the other hand, had the same initial values as the CH4 experiment but did not converge towards the best track results at the final time. The average track error for the CTL experiment was 36.69 km, while the average track error from the CH4 experiment was 23.36 km. These results show that the CH4 assimilation experiment produced a better analysis of Rita's track over the period under consideration. .

b. Tropical Cyclone Intensity Forecast

After examining track results, the performance of the experiments in the forecast of Hurricane Rita's intensity was evaluated. Maximum wind forecasts for the CTL and CH4

experiments were compared to the maximum wind results for the best track at 3 hour intervals. The results are shown in figure 2 below.

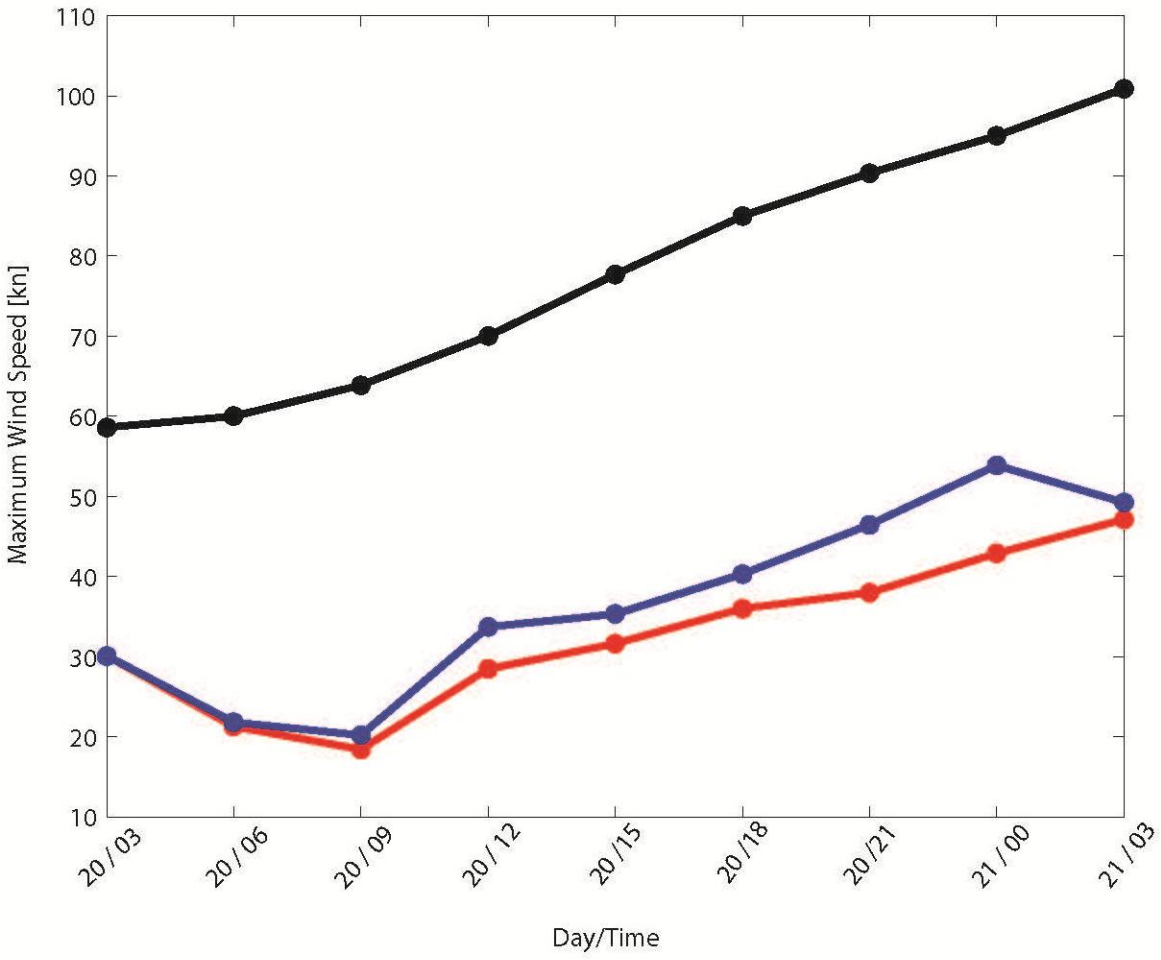

Figure 2. Maximum wind speed forecast in knots (kn) for best track data in black, CTL experiment in red, and the CH4 experiment in blue

The best track values were interpolated with the same method used to make the track figure above. From the figure, it is apparent that the CTL and CH4 results are somewhat similar but are both significantly below the best track results. The best track

results are two times greater than the results obtained from our simulations. This large discrepancy is partly due to the fact that this was a coarse-resolution simulation and intensity was not assimilated. In addition, taking the intensity from the ensemble mean gives a somewhat greater underestimate than taking the mean of the intensities of the individual members. Despite the fact that this was not a high resolution experiment, it is evident that the intensity errors for the CH4 brightness temperature assimilation experiment are significantly lower than the intensity errors for the CTL, which is very encouraging. Maximum wind speed RMS errors were 7.82 kn for the CTL experiment and 4.82 kn for the CH4 experiment, which shows marked improvement. It is also interesting to note that the CH4 experiment produced a better simulation of the intensification that took place from15Z SEP 20 to 0Z SEP 21.

c. Tropical Cyclone Structure Representation

After comparing track and intensity errors, it was appropriate to compare the observation and simulation results for the CH4 experiment at the beginning, middle and end of the assimilation window in order to assess the overall impact of the assimilation of brightness temperatures in the representation of the TC structure. Figure 3 shows the CTL, CH4 experiment simulation, and observation results, in columns 1, 2 and 3 respectively. The data is plotted for three different times: 03Z SEP 20 in row 1, 18Z SEP 20 in row 2, and 12Z SEP 21 in row 3.

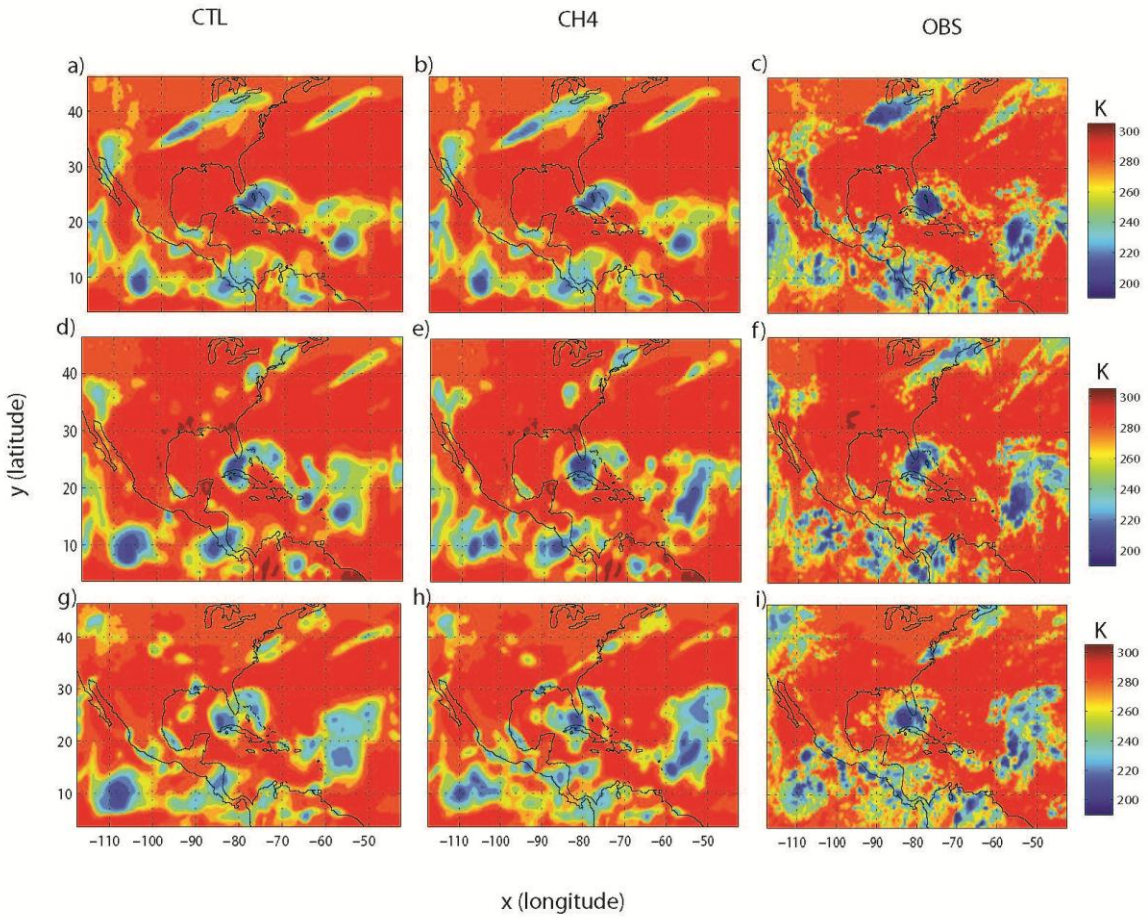

Figure 3. CTL, simulation, and observation results of GOES Channel 4 T_B (˚K) at the beginning, middle, and end of the assimilation window. GOES Channel 4 CTL data is plotted in column 1, simulation results are plotted in column 2, and observations are plotted in column 3. The data is plotted for 03Z September 20 (row 1), 18Z September 20 (row 2), and 12Z September 21 (row 3).

Our experiment was not high resolution but, there are still notable improvements in the results. Overall, the CH4 results compare very well to the observation results and present marked improvements over the CTL results. The assimilation of GOES-12 brightness temperatures produces a more realistic TC cloud field relative to the CTL. In addition to this, the brightness temperature structure throughout the rest of the domain also compared well to

the observations. The superior performance of the CH4 experiment is especially evident when comparing the brightness temperature structure produced by both experiments in the Tropical Pacific region. The CTL experiment produced a very large cloud field that is not present in the observations. On the other hand, the CH4 produced a better cloud field due to the fact that it involves the assimilation of GOES-12 observations that are taken at a greater frequency. Observations taken at a greater frequency aid in producing an improved representation of the TC and the environment in the model initial conditions, which eventually leads to produce accurate TC sizes and structures for all times.

The comparison done above for the GOES-12 CH4 T_B field was also done for the GOES 12 channel 3 T_B. The CTL and CH4 observation and simulation results are shown in figure 4, in columns 1, 2, and 3 respectively.

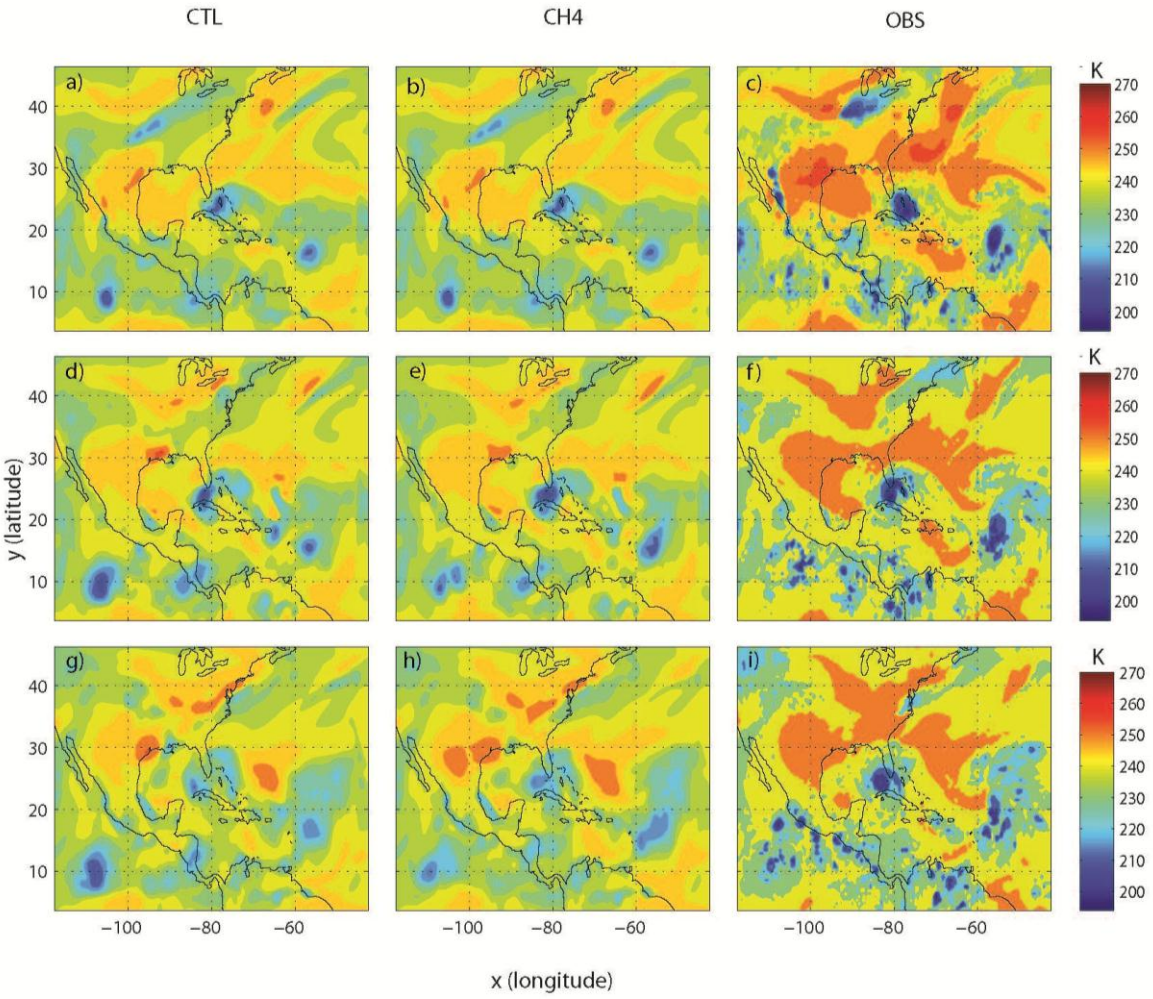

Figure 4. CTL, observation, and simulation results of GOES Channel 3 T_B (˚K) at the beginning, middle, and end of the assimilation window. CTL data is plotted in column 1, simulation results are plotted in column 2, and observations are plotted in column 3. The data is plotted for 03Z September 20 (row 1), 18Z September 20 (row 2), and 12Z September 21 (row 3).

Even though GOES-12 channel 3 data were not assimilated, the assimilation of GOES channel 4 T_B produced improvements in the simulated results of GOES channel 3 T_B. As in

the case of the CH4 T_B, the simulation produced TC sizes and structures similar to what was produced by the observations. The brightness temperature structure produced throughout the rest of the domain also compared well to the observed. So far, the results have shown that the assimilation of GOES CH4 T_B produces remarkable improvement in the TC representation and this improved representation leads to a better forecast of track and intensity. Improvements can still be made with the use of other techniques to reduce some of the noise evident in the assimilation results. However, these techniques will not be discussed since the focus of this paper is to show the potential of the assimilation of GOES-12 CH4 T_B in the representation of TC structure. In the remainder of this paper, the impacts of the assimilation on all the simulated fields will be quantitatively assessed and discussed.

d. Microphysical Fields Representation

A microphysical field, precipitable water content, was also selected to determine if the relationship between reflectivity and microphysics leads to an improved representation of microphysical fields. The differences between the CTL and CH4 results for each field were examined. Results are shown in figure 5. The figures were made by subtracting the CTL results from the CH4 and plotting these differences. The u and v wind components were plotted for the 1176m level. CTL SLP was contoured over each field from 970-1030hPa at 5hPa intervals to determine the location of the storm center and determine how well the assimilation performed in the storm center.

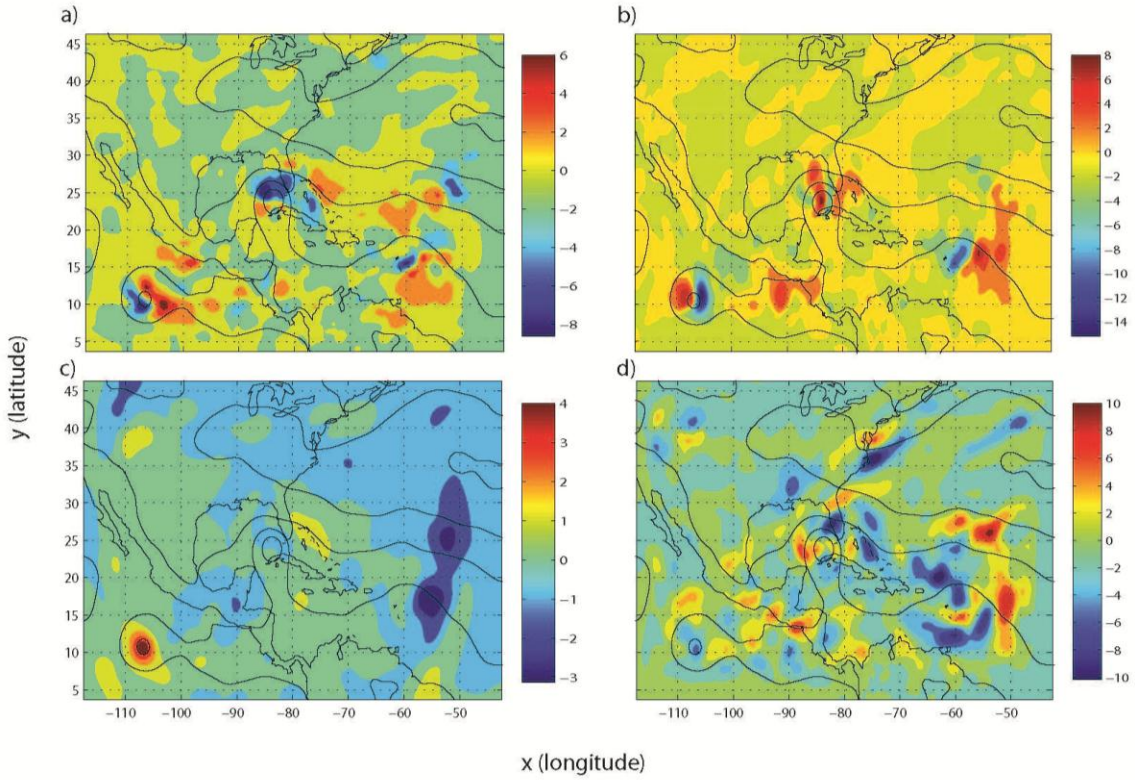

Figure 5. CTL and CH4 differences for u wind component at 1176m height (a), v wind component at 1176m height (b), SLP (c), and Precipitable Water (d). SLP for the CTL experiment was contoured over each field from 970-1030m at 5m intervals.

Overall, the results of the CTL and CH4 experiments are very similar upon examining the differences. The CH4 experiment performed very well in the case of SLP. There is very little difference between the CTL and CH4 results, especially in the TC center. It is interesting to note that in the lower left hand portion of the SLP figure, the CTL had produced a spurious cyclone, which disappeared upon assimilation. Spurious TC genesis is often a problem with numerical weather predictions so this result further supports that the assimilation of GOES brightness temperatures produces results that compare well to the

observations. For the u and v wind components however, the CH4 underestimated the results in certain portions of the storm center. Some localization tuning may be necessary to improve the representation of the u and v wind components.

e. Non-Microphysical Fields Representation

As a final analysis, the RMS error of the ensemble mean for 14 different observed fields was examined to quantitatively assess the overall impact of the assimilation of GOES CH4 T_B on the forecast of each field. The RMS error (RMSE) indicates the forecast error and is defined as follows:

$$RMSE = \sqrt{\frac{1}{D}\sum_{d=1}^{D}\left(x_f^d - x_a^d\right)^2} \quad (4)$$

where x_f^d and x_a^d are respectively the forecast and analysis values at grid point d, and D is the number of grid points. The RMSE results are summarized in table1. The errors in table 1were calculated as the average RMS errors over all times for each field.

Observation Type	**Experiments**			
	RMS Errors		**Calibration**	
	CTL	CH4	CTL	CH4
Max Wind (kn)	7.82296	4.81562	.7114	.4561
AMV u (m/s)	3.83035	3.88645	.7694	.7819
AMV v (m/s)	3.463313	3.492188	.6903	.7019
SLP (hPa)	1.623869	1.633578	.8133	.8223
RAOB U (m/s)	2.8721	2.89735	.7286	.7551

RAOB V (m/s)	2.8309	2.93345	.7354	.7612
RAOB Z (m/s)	15.19825	14.30715	.4499	.4413
RAOB T (K)	1.1726	1.1366	.7291	.7098
CH3 T_B (K)	6.864388	6.338338	.7626	.7165
CH4 T_B (K)	13.08631	11.54479	.7225	.6773
ACARS U (m/s)	3.533533	3.502156	.8403	.8390
ACARS V (m/s)	1.569522	3.473933	.8230	.8304
ACARS T (K)	1.569522	1.554422	1.0575	1.0516
Vortex Latitude	0.262911	0.122589	.6661	.3229
Vortex Longitude	0.161456	0.146244	.2560	.2511

Table 1. RMS errors ad calibration values averaged over the nine assimilation cycles for each field. Errors for max wind, AMV u, AMV v, RAOB U, RAOB V, RAOB Z, ACARS U, and ACARS V are in m/s. Errors for SLP are in hPa. Errors for ACARS T, RAOB T, CH3 $\boldsymbol{T_B}$, and CH4 $\boldsymbol{T_B}$ are in K.

The CTL performed slightly better in most cases but the CH4 experiment performed significantly better in the maximum wind forecast, as was shown in figure 2 of this paper. This was a very encouraging result, especially since this was not a high resolution assimilation experiment. In addition to this, the CH4 brightness temperature assimilation experiment also performed slightly better than the CTL with respect to the RAOB geo potential heights and temperatures as well as vortex position. The CTL experiment, on the other hand, performed significantly better in capturing the ACARS V wind field. For the most part, however, RMS errors for the CTL and CH4 experiments compared well to each other.

Calibration values were calculated, in addition to the RMS errors, since these also serve as a quantitative measure that further aids in assessing the impact of the assimilation on the results. The calibration is defined as the square of the innovation divided by the square of

the ensemble spread. The innovation and ensemble spread are defined by the following equations:

$$innovation(t) = o_t - H_t\,\mu_f(t) \qquad (6)$$

$$ensemble\ spread = \sqrt{\frac{1}{N}\sum_{n=1}^{N}(x_n - \bar{x})^2} \qquad (7)$$

where o_t is the observation vector, N is the number of ensemble members, x_n is the nth ensemble member, and $\bar{x}$ is the ensemble average. The innovation represents the residual between the observation and forecast while the ensemble spread represents the difference between the ensemble members and ensemble mean. Ideally, the innovation and ensemble spread values are comparable and the calibration value would be close to unity. The calibration was calculated as the average calibration over all times for each field. The results of this calculation are shown on the right side panel of Table 1. In general, the calibration values for the CTL and CH4 experiment compared well to each other. Results show that the CH4 experiment performed exceptionally well in the cases of RAOB and AMV u and v wind components. The CH3 T_B and CH4 T_B calibration results of the CH4 experiment also compare well to the results for the CTL, even though they are slightly lower. The only case where the CTL outperformed the CH4 was maximum winds. Overall, the results of the experiments performed in this study show that the assimilation of GOES-12 brightness temperatures leads to an improved representation of TC structure and simulated fields as well as a better forecast of hurricane track and intensity.

2.6) Conclusions

The results obtained in these experiments have shown that the assimilation of GOES-12 channel 4 brightness temperatures with an EnKF produces track and intensity errors lower than simulations that involve conventional observations only. The temporal continuity of the data produces a more realistic TC structure at the initial time. This improved representation at the initial time allows the simulation to generate more accurate track and intensity forecasts. In addition to this, the assimilation of GOES brightness temperatures produced an improved representation of microphysical and non-microphysical fields. The SLP field shows evidence of the improvement in the representation of non-microphysical fields since the assimilation of GOES T_B eliminated the spurious cyclone that developed in the CTL experiment. Therefore, in addition to producing more accurate track and intensity forecasts, assimilation of GOES T_B shows promise in eliminating the existing numerical weather prediction issues with spurious cyclone genesis.

Improvements can always be made to obtain better assimilation results. One method that is usually employed to improve upon assimilation results and eliminate spurious correlations is covariance localization, which can be done in the horizontal and in the vertical, and in time (Campbell and Bishop, 2009). While horizontal covariance localization was applied in this study, vertical covariance localization may have further aided in improving results. The covariance models that are currently applied are stationary and assume uniformity in the vertical, which is not necessarily true for observations near the surface. As opposed to integrated quantities, near-surface parameters have weaker

connections to the flow components above. Thus, the performance of stationary covariance models can be limited if observations near the surface are incorporated. For this reason, vertical localization may be crucial to obtain more accurate results when the ensemble assimilation involves the use of surface data (Hacker et. al. 2007). This could prove to be especially beneficial in the assimilation of intensity. Experiments involving the application of different localization schemes are currently in progress.

In conclusion, GOES-12 channel 4 micron brightness temperature data shows promise in becoming an alternate method to the use of conventional observations to forecast TC track and intensity. The temporal continuity of this data presents many advantages over the use of conventional observations and may in further understanding TC intensification processes. Even though a higher resolution would have been desirable to perform the experiments in this study, the results obtained are very promising. Therefore, the author encourages the use of GOES-12 channel 4 data in assimilation experiments to forecast TC track and intensity. Further research should be done to continue exploring the potential of the assimilation of radiance data from the different channels on GOES-12.

References

Bernardet, L., L. Nance, S. Bao, B. Brown, L. Carson, T. Fowler, J. Halley Gotway, C. Harrop and J. Wolff , 2010: The HFIP High-Resolution Hurricane Forecast test: overview and results of track and intensity forecast verification, presented at 29th Conference on Hurricanes and Tropical Meteorology, AMS, Tucson, AZ, May 9-14.

Campbell, W. F., Bishop, C. H, and D. Hodyss, 2010: Vertical Covariance Localization for Satellite Radiances in Ensemble Kalman Filters. *Mon*. *Wea*. *Rev*., **138**, 282–290.

Davis, C.,Wang, W., Dudhia, J., and R. Torn, 2010: Does Increased Horizontal Resolution Improve Hurricane Wind Forecasts? *Wea*. *Forecasting*, **25**, 1826–1841.

Emanuel, K. A., 1991: A scheme for representing cumulus convection in large-scale models. *J*. *Atmos*. *Sci*., **48,** 2313–2335.

Evensen, G., 1994: Sequential data assimilation with a nonlinear quasi-geostrophic model using Monte Carlo methods to forecast error statistics. J Geophys Res, **99C**, 10143–10162

Evensen, G., 2003: The ensemble Kalman filter: Theoretical formulation and practical implementation. *Ocean Dynamics*., **5**, 343–367

Evensen, G., 2004: Sampling strategies and square root analysis schemes for the EnKF. *Ocean Dynamics*., **54**,539–560

Gaspari, G., and S. E. Cohn, 1999: Construction of correlation functions in two and three dimensions. *Quart*. *J*. *Roy*. *Meteor*. *Soc*., **125,** 723–757.

Gelb, A., Kasper, J. F., Nash, R. A., Price, C. F., and A. A. Sutherland, 1974: *Applied Optimal Estimation*. M. I. T. Press, 374 pp.

Hacker, J. P., Anderson, J. L., and M. Pagowski, 2007: Improved Vertical Covariance Estimates for Ensemble-Filter Assimilation of Near-Surface Observations. *Mon. Wea. Rev.*, **135**, 1021–1036.

Hamill, T. M., Whitaker, J. S., and C. Snyder, 2001: Distance-Dependent Filtering of Background Error Covariance Estimates in an Ensemble Kalman Filter. *Mon. Wea. Rev.*, **129**, 2776–2790.

Hamill, T. M., 2006: Ensemble-based data assimilation. Predictability of Weather and Climate, T. Palmer and R. Hagedorn, Eds., Cambridge Press, 124–156.

Houtekamer, P. L., and H. L. Mitchell, 1998: Data Assimilation Using an Ensemble Kalman Filter Technique. *Mon. Wea. Rev.*, **126**, 796–811.

Houtekamer, P.L., and H. L. Mitchell, 2001: A Sequential Ensemble Kalman Filter for Atmospheric Data Assimilation. *Mon. Wea. Rev.*, **129**, 123–137.

Kalman, R. E., and R. S. Bucy, 1961: New Results in Linear Filtering and Prediction Theory.

Journal of Basic Engineering., **83**, *95-108*

Koyama, T., Vukicevic, T., Sengupta, M., Haar, T. V., and A. S. Jones, 2006: Analysis of Information Content of Infrared Sounding Radiances in Cloudy Conditions. *Mon*. *Wea*. *Rev*., **134**, 3657–3667.

Lewis, W. E, and G. J. Tripoli, 2006: EnKF assimilation of simulated spaceborne Doppler observations of vertical velocity: impact on the simulation of a supercell thunderstorm and implications for model-based retrievals. *Advances in Geosciences*. **Vol. 7**, pp 343-348

LI, X., and A. PU, 2009: Sensitivity of Numerical Simulations of the Early Rapid Intensification of Hurricane Emily to Cumulus Parameterization Schemes in Different Model Horizontal Resolutions, *Journal of the Meteorological Society of Japan*, Vol. 87, No. 3, 403-421

Lorenc, A.C., 2003: The potential of the ensemble Kalman filter for NWP – a comparison with 4D-Var. *Quart*. *J*. *Roy*. *Meteor*. *Soc*., **129**, 3183–203.

Maybeck, P. S., 1982: Stochastic Models, Estimation, and Control.Vol. 1. Academic Press, 423

Mitchell, H., Houtekamer, P.L., and G. Pellerin, 2002: Ensemble Size, Balance, and Model-Error Representation in an Ensemble Kalman Filter*. *Mon. Wea. Rev.,* **130**, 2791-2808.

Raymond, W. H., Wade, G. S., and T. H. Zapotocny, 2004: Assimilating GOES Brightness Temperatures. Part II: Assigning Water Vapor Wind Heights Directly from Weighting Functions. *J. Appl. Meteor.*, **43**, 1200–1212.

Rogers, R., and Coauthors, 2006: The Intensity Forecasting Experiment: A NOAA Multiyear Field Program for Improving Tropical Cyclone Intensity Forecasts. *Bull. Amer. Meteor. Soc.*, **87**, 1523–1537.

Sadourny, R., and P. Morel, 1969: A Finite-Difference Approximation of the Primitive Equations for a Hexagonal Grid on a Plane. *Mon. Wea. Rev.*, **97**, 439–445.

Snyder, C., and F. Zhang, 2003: Assimilation of Simulated Doppler Radar Observations with an Ensemble Kalman Filter. *Mon. Wea. Rev.*, **131,** 1663–1677.

Tippett, M. K., Anderson, J. L., Bishop, C. H., Hamill, T. M., and J. S. Whitaker, 2003: Ensemble Square Root Filters*. *Mon. Wea. Rev.*, **131**, 1485–1490.

Torn, R. D., and G. J. Hakim, 2009: Ensemble Data Assimilation Applied to RAINEX

Observations of Hurricane Katrina (2005). *Mon*. *Wea*. *Rev*., **137**, 2817–2829.

Toth, Z., Zhu, Y., and T. Marchok, 2001: The Use of Ensembles to Identify Forecasts with Small and Large Uncertainty. *Wea*. *Forecasting*, **16**, 463–477.

Tripoli, Gregory J., 1992: A Nonhydrostatic Mesoscale Model Designed to Simulate Scale Interaction. *Mon*. *Wea*. *Rev*., **120**, 1342–1359.

Whitaker, J. S., and T. M. Hamill, 2002: Ensemble Data Assimilation without Perturbed Observations. *Mon*. *Wea*. *Rev*., **130**, 1913–1924.

Zhang, F., Snyder, C., and J. Sun, 2004: Impacts of Initial Estimate and Observation Availability on Convective-Scale Data Assimilation with an Ensemble Kalman Filter. *Mon*. *Wea*. *Rev*., **132**, 1238-1253

Zhang, F., and C. Snyder, 2007: Ensemble-Based Data Assimilation. *Bull*. *Amer*. *Meteor*. *Soc*., **88**, 565–568.

Zhang, F., Weng, Y., Sippel, J. A., Meng, Z., and C. H. Bishop, 2009: Cloud-Resolving Hurricane Initialization and Prediction through Assimilation of Doppler Radar Observations with an Ensemble Kalman Filter. *Mon*. *Wea*. *Rev*., **137**, 2105–2125.

Chapter 3

Bogussing Methods for Quantification of Uncertainties in the Tropical Cyclone Vortex Structure

Environmental flow and tropical cyclone vortex structure are the two main factors that determine tropical cyclone motion. Of these two factors, environmental steering is the most important as it can explain a large part of the TC motion, especially when the flow is strong. Studies by Fiorino and Elsberry (1989) have demonstrated that TC motion is not very sensitive to the intensity and inner-core structure, but depends more on the outer-core velocity profile. The fact that TC track is not very dependent on vortex structure has a positive impact on TC track forecasting. The NHC reports that improvement in 24–72-h track forecast errors for the Atlantic basin have been reduced by about 50% in the last 15 years (Franklin, 2010). This accomplishment in TC track forecasting would not be possible if cyclone motion were highly dependent on vortex structure as TC inner core structure cannot be determined accurately from the sparse observations over the tropical oceans. Heavily relying on vortex structure to forecast track would introduce a significant amount of error into TC track forecasts.

The limited sensitivity of TC motion to vortex structure is what led to the improved track forecast (over the intensity forecast) in the experiments discussed in Chapter 2. The experiments described in Chapter 2 focused on perturbing only the environment to create an

ensemble of initial conditions that were employed to initialize the model. Therefore, the ensemble mean provided a better estimate of TC track than each ensemble member individually while the ensemble spread provided a measure of the uncertainty in the environmental flow. While producing an accurate forecast is always important and is the main goal, knowledge of the uncertainty associated to the factors that determine TC motion is also essential as this will help determine the confidence that can be attributed to such a forecast.

Although the environmental flow uncertainty was determined in the set of experiments described in Chapter 2, the methods that were employed do not provide information about the uncertainty associated with the TC vortex structure. Accurately representing TC structure in the model initial conditions has always been a challenge. The lack of observations over the ocean surface and the near the TC core region makes it difficult to capture detail in the tropical cyclone structure and produce a realistic vortex. Initial vortices produced by the large scale analysis from operational centers are weak, poorly defined, and in some cases misplaced (Zou, 1999). Small errors in vortex position, motion, strength, and environmental flow can lead to inaccurate short-term forecasts of TC track and intensity (Kurihara et al. 1993). High resolution experiments have been implemented in an attempt to address this issue but have proven that due to the difficulty of observation, it is not certain whether the accurate structure of the TC is available at higher resolution (Kwon, 2009). Consequently, employing a method that remedies issues with sparse observations in the TC vortex as well as quantifies the uncertainty associated with the vortex structure is crucial.

While improving vortex structure representation and quantifying the uncertainty associated with it is important for determining TC motion, it is even more important for TC intensity forecasting. Shortcomings in the collection of TC inner-core data makes it difficult to provide real-time estimates of TC structure and intensity to forecasters and for assimilation into the NWP models. Limitations in observing capabilities near the TC inner core are one of the main reasons that have contributed to the limited improvement in TC intensity forecasting skill (Rogers, 2006). Therefore, to have any hope of accurately simulating TC intensity, issues with sparse observations need to be addressed as data assimilation methods by themselves (without enough observations) are not sufficient to produce significant improvement in TC intensity forecasts.

One method that has been implemented by the Geophysical Fluid Dynamics Laboratory (GFDL) to get past issues with sparse observations is the "bogus" vortex method. The GFDL bogussing method involves substituting the original weak vortex from the large-scale analysis with a more realistic synthetic vortex. To remove the poorly resolved vortex from the large scale-analysis, two spatial filters are applied. The specified vortex to be placed in the environmental field consists of a symmetric vortex and an asymmetric flow. The symmetric component is generated from a time integration of an axisymmetric version of the hurricane prediction model, with an observationally derived constraint imposed on the tangential flow. The generated symmetric wind is used in the computation of the asymmetric component using a simplified barotropic vorticity equation, thus providing consistent symmetric and asymmetric components. The mass field is then recomputed using a static initialization method in which the generated wind field is not modified. This TC bogussing

initialization method has led to significant success when applied in operational TC forecasting (Kurihara et al. 1993, 1995; Bender et al. 2007). It has also significantly improved the accuracy of TC track and intensity predictions (Thu and Krishnamurti 1992; Serrano and Unde´n 1994; Leslie and Holland 1995; Bender et al. 2007).

More recently, a new approach to the TC bogussing initialization method denominated bogus data assimilation (BDA) has been developed. This method uses a four-dimensional variational data assimilation (4DVAR) technique in combination with the bogus surface pressure (Zou and Xiao 2000; Pu and Braun 2001; Zhang et al. 2007; Wang et al. 2008). BDA suppresses the incorporation of the synthetic vortex to a minimum while producing a TC with variables that are dynamically and physically balanced. When compared to cases without TC initialization, forecasts with BDA have shown improvement in both intensity and structures representation of TCs.

Besides showing promise in solving issues with limited observations, bogussing methods also allow quantification of the uncertainty associated with the TC vortex structure when applied in ensemble forecasting. According to Cheung and Chan (1998), the addition of such a vortex can be viewed as part of the model configuration. Consequently, an ensemble that is created by perturbing the bogus vortex can sample the vortex uncertainties better when compared with the methods that create an ensemble by perturbing the environmental flow. The idea behind the bogussing method is “to consider how errors in the observed quantities (e.g., position and intensity) are transferred to the various components of the vortex”, as was pointed out by Cheung and Chan (1998).

Although results obtained in BDA studies have been successful, Kwon and Cheong argue that detail in the structures of BDA simulated TCs suggests that the results would improve if a bogus vortex of a realistic three-dimensional structure were applied (Kwon and Cheong, 2010). Such scheme to produce a bogus vortex of a three-dimensional structure for TC track and intensity predictions was implemented by Kwon and Cheong (2010). This scheme is similar to the GFDL bogus initialization method. However, it employs a different method to derive the radial profiles of the surface pressure and tangential wind and to derive the asymmetric component (beta gyre), which are the most important factors to derive the TC initial structure. In their scheme, a spherical high-order filter with double-Fourier series capable of giving a sharp cutoff is applied to split the disturbance from the basic field in the global analysis. In addition to this, empirical formulas for the variables in the axisymmetric components are also employed. Kwon and Cheong indicate that making such modifications to bogus and BDA schemes are possible as long as the qualitative structure of the TC (rather than the detailed structure) is thought to be important as the initial condition.

Kwon and Cheong's bogus TC initialization scheme has proven to be successful in the study of typhoons in the North Pacific and East China during the year 2007. In their study, track errors improved over forecasts without TC initialization by 46%, improvements over the operational center at RSMC were of 49%, and errors of minimum SLP were reduced by 55% compared to the operational forecasts of RSMC (Kwon and Cheong, 2010). Such feats make this scheme attractive for application in ensemble forecasting schemes and thus will be applied in our study.

The focus of the next series of data assimilation experiments will change from the environmental flow to the TC vortex structure. A bogussing method implemented by Kwon and Cheong is applied for TC initialization and the ensemble members are created via perturbations of the TC vortex structure. GOES-12 channel 4 10.7 micron brightness temperature observations will be assimilated as well as GOES-12 channel 3 water vapor observations. It is expected that GOES data in combination with the Kwon and Cheong bogussing method will lead to an improved representation of TC structure, which will hopefully lead to an improved forecast of TC track and intensity. The next chapter discusses the details of the experiments and also presents results.

References

Bender, M. A., I. Ginis, R. Tuleya, B. Thomas, and T. Marchok, 2007: The operational GFDL coupled hurricane–ocean prediction system and a summary of its performance. Mon. Wea. Rev., 135, 3965–3989.

Chan, J. C. L. and K. K. W. Cheung, 1998: Characteristics of the asymmetric circulation associated with tropical cyclone motion. *Meteor. Atmos. Phys.*, 65, 183-196.

Fiorino, M., and R. L. Elsberry, 1989: Some aspects of vortex structure related to tropical

cyclone motion. *J*. *Atmos*. *Sci*., **46,** 975–990.

Franklin, J. F., cited 2010: 2009 National Hurricane Center forecast verification report. [Available on line at http://www.nhc.noaa.gov/verification.]

Kurihara, Y., M. A. Bender, and R. J. Ross, 1993: An initialization scheme of hurricane models by vortex specification. Mon. Wea. Rev., 121, 2030–2045.

Kurihara, Y., M. A. Bender , R. E. Tuleya, and R. J. Ross, 1995: Improvements in the GFDL hurricane prediction system. Mon. Wea. Rev., 123, 2791–2801.

Kwon, In-Hyuk, Hyeong-Bin Cheong, 2010: Tropical Cyclone Initialization with a Spherical High-Order Filter and an Idealized Three-Dimensional Bogus Vortex. *Mon*. *Wea*. *Rev*., **138**, 1344–1367

Leslie, L. M., and G. J. Holland, 1995: On the bogussing of tropical cyclones in numerical models: A comparison of vortex profiles. Meteor. Atmos. Phys., 56, 101–110.

Pu, Z. X., and S. A. Braun, 2001: Evaluation of bogus vortex techniques with four-dimensional variational data assimilation. Mon. Wea. Rev., 129, 2023–2039.

Serrano, E., and P. Unde´ n, 1994: Evaluation of a tropical cyclone bogussing method in data assimilation and forecasting. Mon. Wea. Rev., 122, 1523–1547.

Thu, T. V., and T. N. Krishnamurti, 1992: Vortex initialization for typhoon track prediction. Meteor. Atmos. Phys., 47, 117–126.

Wang, D., X. Liang, Y. Zhao, and B. Wang, 2008: A comparison of two tropical cyclone bogussing schemes. Wea. Forecasting, 23, 194–204.

Zhang, X., Q. Xiao, and P. J. Fitzpatrick, 2007: The impact of multisatellite data on the initialization and simulation of Hurricane Lili's (2002) rapid weakening phase. Mon. Wea. Rev., 135, 526–548.

Zou, X., and Q. Xiao, 2000: Studies on the initialization and simulation of a mature hurricane using a variational bogus data assimilation scheme. J. Atmos. Sci., 57, 836–860.

Chapter 4

Assimilation of GOES-12 Brightness Temperatures and Water Vapor Observations with an EnKF and Bogus Vortices for Simulations of Tropical Cyclone Rita

4.1) Introduction

In the first part of this study (Chapter 2), an EnKF scheme was applied to assimilate GOES-12 channel 4 10.7 micron brightness temperatures and produce track and intensity forecasts for Tropical Cyclone Rita. The performance of the scheme in the representation of TC structure, microphysical, and non-microphysical fields was also examined. In this EnKF scheme, the ensemble members were created via perturbations of the environment. Therefore, the ensemble mean provided a better estimate of TC track and intensity than each ensemble member individually while the ensemble spread provided a measure of the uncertainty in the environmental flow. The most interesting of the result was the elimination of the spurious cyclone upon assimilating GOES-12 channel 4 brightness temperatures. Although the experiments were performed at a coarse resolution of 60 km, results showed that the assimilation of GOES-12 brightness temperatures with an EnKF scheme shows potential in improving TC forecasts and eliminating issues with spurious cyclones.

However, a significant downside of the experiments performed in Chapter 2 is that they do not provide a measure of uncertainty in the TC vortex structure, which is useful for TC intensity forecasting. Observing capabilities are extremely limited in the region of the

tropical cyclone vortex, which makes it difficult to produce an accurate representation the TC inner core structure in the model initial conditions. The inability to accurately represent TC structure in model initial conditions is one of the main reasons that explains the limited improvement in TC intensity forecasting (Rogers, 2006) as changes in storm intensity are driven by highly variable, small scale dynamics internal to the storm. Given the sparse amount of observations that sample the TC inner core, a measure that quantifies the uncertainty associated with these observations is useful. Employing a method that treats issues with sparse observations and allows ensemble members to capture different possible states of the TC vortex structure may aid in improving TC intensity forecasts.

One method that has been implemented to treat issues with sparse observations is the "bogus" vortex method (Kurihara et al. 1993, 1995). This method is applied by the Geophysical Fluid Dynamics Laboratory (GFDL) and involves substituting the original weak vortex from the large-scale analysis with a more realistic synthetic vortex. This GFDL bogussing initialization method has successfully been applied to operational forecast of TCs (Kurihara et al. 1993, 1995; Bender et al. 2007). It has also significantly contributed to improving the accuracy of TC track and intensity forecasts (Thu and Krishnamurti 1992; Serrano and Unde´n 1994; Leslie and Holland 1995; Bender et al. 2007).

More recently, a new approach to the TC bogussing initialization method denominated bogus data assimilation (BDA) has been developed. This method uses a four-dimensional variational data assimilation (4DVAR) technique in combination with the bogus surface pressure (Zou and Xiao 2000; Pu and Braun 2001; Zhang et al. 2007; Wang et al. 2008). The

object of this method is to suppress the incorporation of the synthetic vortex to a minimum while producing TCs with variables that are dynamically and physically balanced. When compared to cases without TC initialization, forecasts with BDA have shown improvement in both intensity and structures of TCs. Some researchers (Kwon and Cheong) argue, however, that the detail in the structure of the TCs simulated with BDA could improve with a bogus vortex of a realistic three-dimensional structure (Kwon and Cheong, 2010).

Such scheme to produce a bogus vortex of a three-dimensional structure for TC track and intensity predictions was implemented by Kwon and Cheong (2010). This scheme is a variant of the GFDL method with certain modifications made to the method to derive the radial profiles of the surface pressure and tangential wind and to derive the asymmetric component (beta gyre), as discussed in Chapter 3. Kwon and Cheong's bogus TC initialization scheme has proven to be successful in the study of typhoons in the North Pacific and East China during the year 2007. The improvement produced by their scheme in the reduction of errors in track and minimum SLP over RSMC and forecasts without TC initialization makes this method attractive for application in ensemble forecasting schemes and thus was chosen for our study.

In this study, the Kwon and Cheong TC initialization bogussing method is applied in conjunction with the EnKF to assimilate GOES-12 channel 4 10.7 micron brightness temperatures and simulate tropical cyclone Rita. It is hypothesized that applying the Kwon and Cheong TC bogussing scheme in conjunction with the continuous assimilation of GOES-12 brightness temperatures will lead to an improved representation of TC structure in the

model initial conditions. With an improvement in TC structure representation at the initial time, improved forecasts and predictability of track and intensity are also expected.

In addition to the experiment described above, a separate experiment is performed where GOES-12 channel 3 water vapor observations are assimilated. Moisture sensitive channels on GOES (as well as temperature sensitive channels) are useful for assimilation in clear sky conditions and also in the presence of optically thin to moderate high level clouds as was shown by Koyama et. al.(2006). Results from their study showed that the use of infrared sounding observations in data assimilation could improve temperature and humidity profiles below optically thin-moderate ice clouds. Although Koyama employed GOES sounder observations instead of GOES imager observations, it is expected that assimilating GOES-12 imager water vapor observations will have a positive impact on TC structure representation, track and intensity. Results for this experiment will be compared to the brightness temperature assimilation experiment to determine which observations lead to a more significant improvement.

The details of the experiments in this chapter are described in the following sections. Section 4.2 discusses (a) the model configuration, (b) observations, (c) TC initialization, as well as (d) the methodology to generate perturbations of the TC vortex and (e) assimilate GOES data. Section 4.3 presents the results obtained from the analysis and discussion. These include the results for (a) track forecasts, (b) intensity forecasts, (c) TC structure representation, (d) microphysical field representation, (e) non microphysical field representation. Finally, Section 4.4 presents conclusions and future work.

4.2) Methodology

The objective of this research is to build upon the study described in Chapter 2 and further explore the potential of a GOES-12 brightness temperature assimilation scheme to improve TC track, intensity, and structure representation. Certain modifications were made to the methodology described in Chapter 2 to determine if further improvement can be obtained. The modifications that were made to the methodology are directed towards improving the representation of the TC structure. Hopefully this will lead to more accurate forecasts of TC track and intensity.

The first modification made in this study was to the method employed for TC initialization and to create the ensemble of analyses. In Chapter 2, the ensemble members were created via perturbation of the environment. In this study, a bogussing method is applied for TC initialization and the ensemble members are now created via perturbation of the TC vortex. The idea behind this approach is that this will allow better quantification of the uncertainty in the TC vortex structure. Knowledge of this uncertainty is essential given the difficulties in observing capabilities near the TC core.

In addition to modifying the TC initialization and the method employed to create the ensemble members, the experiments in this study are run at a higher resolution of 18km. In Chapter 2, the experiments were run at a coarse resolution of 60km. A full analysis of the TC track, intensity, structure representation, as well as representation of microphysical and non-microphysical fields was done with the results of the low resolution run as a sensitivity test.

More importantly, the low resolution experiments performed in Chapter 2 were essential to determine the forecast bias in the GOES CH3 and CH4 observations, which was employed to perform bias correction in respect to the CH3 and CH4 observations in the high resolution experiments of this chapter. With a higher resolution, now it is possible to better resolve the TC core, which allows examination of mesoscale features in more detail.

As in Chapter 2, the EnKF is used to assimilate conventional (RAOB, METAR, ACARS, etc.) and GOES-12 brightness temperatures (T_B) observations to improve the representation, track, and intensity forecasts for Hurricane Rita. A control experiment (CTL) with conventional observations only and a CH4 experiment, which assimilates both conventional and GOES-12 channel 4 brightness temperatures, are performed in this study. The differences between results from the experiments were then examined to determine how the assimilation of GOES brightness temperatures impacts the forecast. In addition to the CTL and CH4 experiments, a third experiment assimilating GOES-12 channel 3 water vapor observations (CH3) is also performed. Further details on this third experiment are discussed later on. Details on the methodology employed in this study are presented below.

a. *Model Configuration*

The UW-NMS was initialized on a domain employing 40, 200 and 150 grid points respectively in the vertical, zonal and meridional directions. The grid spacing was of 18-km in the horizontal directions and 300-m stretched to 700-m in the vertical direction. A time step of 60s was used to integrate the model forward. The bulk microphysics scheme applied

uses two liquid (rain, cloud water) and two ice (snow, pristine crystals) species with a single-moment scheme (Tripoli, 1992). A covariance relaxation factor of 0.2 was applied.

b. *Observations*

Three different experiments were performed in this study. The two main experiments are the control (CTL), which incorporates conventional observations only, and the CH4 experiment, which incorporates GOES channel 4 brightness temperatures in addition to conventional observations. However, a third experiment, denominated CH3, is performed in this study, and involves the assimilation of GOES-12 channel 3 water vapor data and conventional observations.

The CTL experiment incorporates METAR (SLP), Aircraft Communication Addressing and Reporting System (ACARS (u, v, T)), RAOB (u, v, T, T_d), and POES (retrieved T, T_d) data obtained from the meteorological assimilation data ingest system (MADIS); and Vortex Information (lat, lon of TC center) data obtained from the TC VITALS. Cloud drift winds (AMV (u, v)) from GOES-11 and GOES-12 are also employed. Different from the CTL experiment in chapter 2, this experiment also assimilated vortex maximum surface winds in knots. The errors used for the conventional data are the NCEP Global Data Assimilation System (GDAS) values.

The CH4 experiment incorporates the GOES-12 Channel 4 10.7 micron brightness temperature data (thinned to 120km), which was retrieved from the NOAA Comprehensive

Large Array-data Stewardship System (CLASS). An observation error of 10K was used in this study.

The CH3 experiment incorporates the GOES-12 channel 3 6.5 micron water vapor observations, which were also retrieved from NOAA CLASS. An observation error of 2.5K was used.

c. *TC Initialization Bogussing Method*

The TC initialization method employed for this experiment is similar to that employed by Kwon and Cheong (2010). In summary, The Kwon and Cheong TC initialization method consists of four steps: 1) Input of the Regional Specialized Meteorological Center (RSMC) information and splitting of the global analysis data into basic field and disturbance, 2) determining TC domain in the disturbance field, 3) design of an idealized three-dimensional axisymmetric vortex, and 4) merging the axisymmetric vortex with the disturbance within the TC domain, and modification of the relative humidity (Kwon and Cheong, 2010). However, instead of using RSMC information as Kwon and Cheong did in step 1, tropical cyclone vitals (TcVitals) were employed for the purpose of our study.

Kwon and Cheong's TC initialization method is a variant of Kurihara's GFDL initialization method (Kurihara et. al. 1993, 1995). While the first two steps are very similar to what is done in the GFDL initialization, the third step is unique to Kwon and Cheong's

study. To avoid any confusion, Kwon and Cheong's initialization method will be referred to hereafter as KC initialization method.

The KC TC initialization methodology was chosen over the GFDL's methodology due to the encouraging results obtained by Kwon and Cheong in their 2010 study. They implemented and employed such initialization method to produce forecasts of track and intensity of typhoons observed in 2007 over the western North Pacific and East China. From their study, track errors improved over forecasts without TC initialization by 46%, improvements over the operational center at RSMC were of 49%, and errors of minimum SLP were reduced by 55% compared to the operational forecasts of RSMC (Kwon and Cheong, 2010). There are a few factors in the KC initialization methodology, different from the GFDL's, that led to these improved results and thus were of interest for the purpose of our study.

The first factor is the balance among variables that is taken into account during the construction of the three dimensional bogus vortex to maintain gradient wind balance, hydrostatic balance, and mass balance. All the variables of the bogus vortex are determined in analytic functions on input of the basic four parameters provided by TcVitals best track data: central pressure, positions of the TC center, radial distances of tangential wind of 30kt, and the maximum wind. However, two additional parameters, ambient mean surface pressure and the averaged temperature at the surface pressure level, are added to the TcVitals parameters to match the data over which the bogus vortex replaces the disturbance field. These six parameters explicitly include the information about the size and intensity of the storm. This leads the bogus vortex to accurately reproduce important features that are

specific to the tropical cyclone of interest. Imbalances among variables of the bogus vortex can cause abrupt changes in TC intensity, which would cause systematic bias in the forecast model (Kwon and Cheong, 2010).

Finally, the second factor that led to the improved results in Kwon and Cheong's study is the method that was employed to specify the radial flow. Usually, the radial flow in TC initializations is obtained through the time integration of an axisymmetric model with tangential wind forcing (Iwasaki et. al. 1987, Kurihara et. al. 1993, 1995).In this study, the radial flow is determined empirically based on observations. An appropriate specification of the radial flow that maintains mass balance is believed to facilitate vertical motion, especially near the center of the TC. In the absence of either the inflow or outflow, the vertical motion may not be sufficiently organized into the magnitude necessary to develop the TC. The authors (Kwon and Cheong) believe that the success of their scheme for the TC track and intensity prediction in a variety of ranges in horizontal scales and intensity seems to have been achieved by the flexibility of the bogus vortex whose vertical and horizontal scale are specified automatically upon input of the TcVitals information.

Although Kwon and Cheong's TC initialization methodology proved to be successful for their study, a slightly different approach was taken in this study to separate the disturbance from the global analysis. For the purpose of this study, the scale separation was done with the method employed by GFDL. In the GFDL method, the scale separation is done by filtering the horizontal two dimensional grid point data with a digital filter, which consists of a three – point spatial operator. It is a one dimensional spatial operator that is applied to the zonal direction first and then to the meridional direction. The KC method, on the other hand,

employs a sharp cutoff filter for the splitting of the disturbance from the basic field in the global analyses. The spectral filter applied in the KC method is isotropic on the spherical surface since it gives the same damping rate for the disturbances of a certain horizontal scale regardless of their meridional locations. As the filter order increases, a sharper splitting of the global analysis is achieved. While a sharp-cutoff filter is useful in cases where a global spectral model is employed (as in Kwon and Cheong's study), the GFDL method is easier apply in cases where a regional model in being employed (as in our study).

d. *Perturbations of the TC vortex to create and Ensemble of Analyses*

The ensemble of analyses was created by perturbing maximum velocity, latitude, and longitude deterministically. Maximum velocity perturbation values that were used are -7, -5, 0, 5, 7 kn while -1, 0, and 1 degrees were used for latitude and longitude. The ensemble of initial conditions was created using all possible combinations of these values.

e. *Assimilation of GOES-12 Brightness Temperatures*

The method to assimilate GOES-12 channel 4 brightness temperatures was the same that was used in Chapter 2. This procedure is discussed in Section 2.3 e) of Chapter 2.

4.3) Results and Discussion

Eight total assimilation cycles were performed to assess the impact of the assimilation of GOES-12 channel 4 brightness temperatures on the simulation of tropical cyclone Rita

during the time period between 15Z SEP 20 and 12Z SEP 21. As opposed to the experiments from Chapter 2, these experiments were performed at an 18km resolution and the ensemble members were created via perturbations of the TC vortex. Although the methodology applied in this study is different than that of Chapter 2, the methods employed to analyze the results are similar. First, the impact of assimilating brightness temperatures on the simulation of TC track, intensity, and TC structure is discussed. Then, the performance of the CH4 experiment on the representation of non-microphysical and microphysical fields is examined by comparisons of the ensemble mean solutions of the CTL and CH4 experiments and root-mean-square (RMS) analysis error. The impact of assimilating water vapor observations (CH3 experiment) is also discussed.

a) *TC Track Forecast*

In this section, the track forecast of the CH4 and CTL experiments are analyzed to determine how well the results compared to the positions given by the best track. As in the experiments of Chapter 2, the best track data was only available at 6 hour intervals from 0Z SEP 20 to 12Z SEP 21 while the CTL and CH4 data was available at 3 hour intervals from 03Z SEP 20 to 12Z SEP 21. Therefore, the best track data was interpolated with splines at 3 hour intervals so the times matched those of the CTL and CH4 experiments. The results obtained for the track forecast are shown in Figure 1 with the best track data in black, CH4 data in blue, and CTL in red.

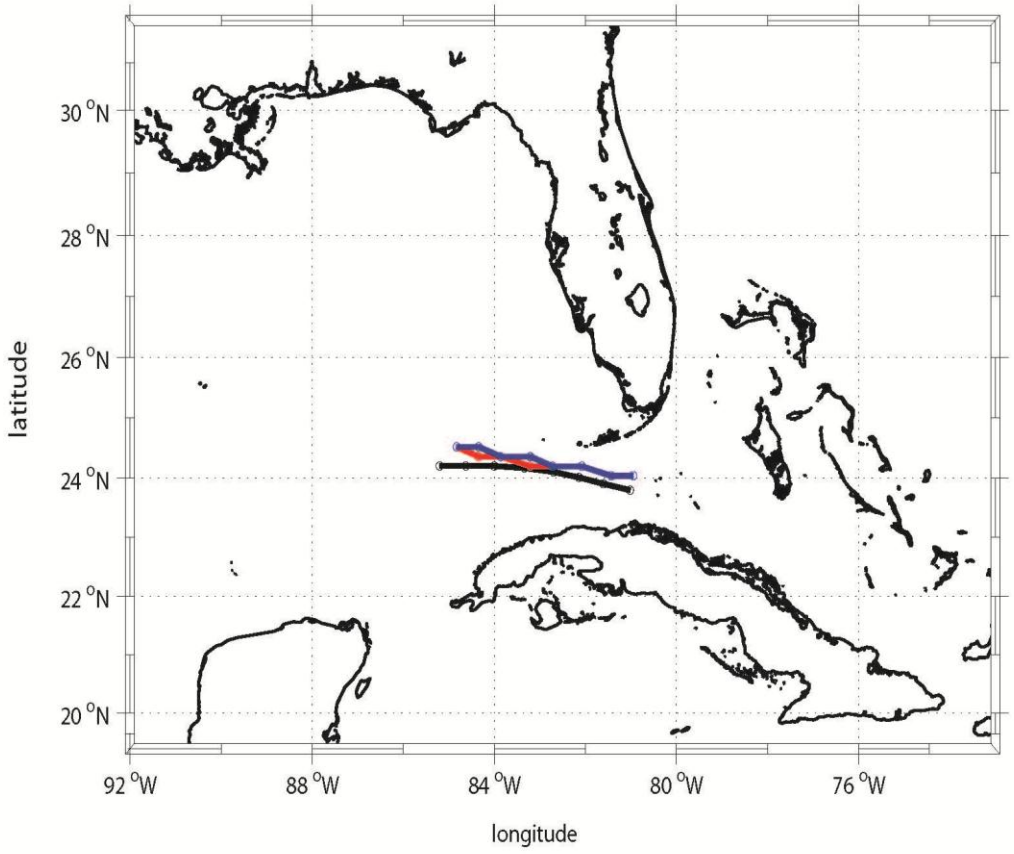

Figure 1. Track forecast for best track data in black, CTL experiment in red, and the CH4 experiment in blue. The data is plotted at 3 hour intervals from September 20 15Z-September 21 12Z.

The track forecasts for both, the CTL and CH4 experiment, do not compare well to the positions given by the best track. Although the initial times for both experiments were similar to that of best track, the results do not converge to the same position as the best track during the final time. There is only one occasion where the CTL converges to the same position as the best track, which was at 0Z on SEP 21. The CH4 experiment never converges to the same

positions as the best track. Overall, the CTL positions compare better to the best track. The average track error of the CTL is 26.57 km while the CH4 average track error is of 29.38 km.

It is interesting to note, however, that although the CTL experiment produced a better track forecast than the CH4, there were only two times where the values give by the CTL were different from that of the CH4 simulation. The CTL and CH4 positions were the same at the first four times (not shown) and they also converged to the same value at the sixth and final time. The positions at the fifth and seventh time were what led to the improved results of the CTL over the CH4.

The track forecast from the CH3 experiment was also compared to the positions given by CTL and best track for the same time period. The results are shown below in Figure 2 with the best track in black, CH3 in blue, and CTL in red.

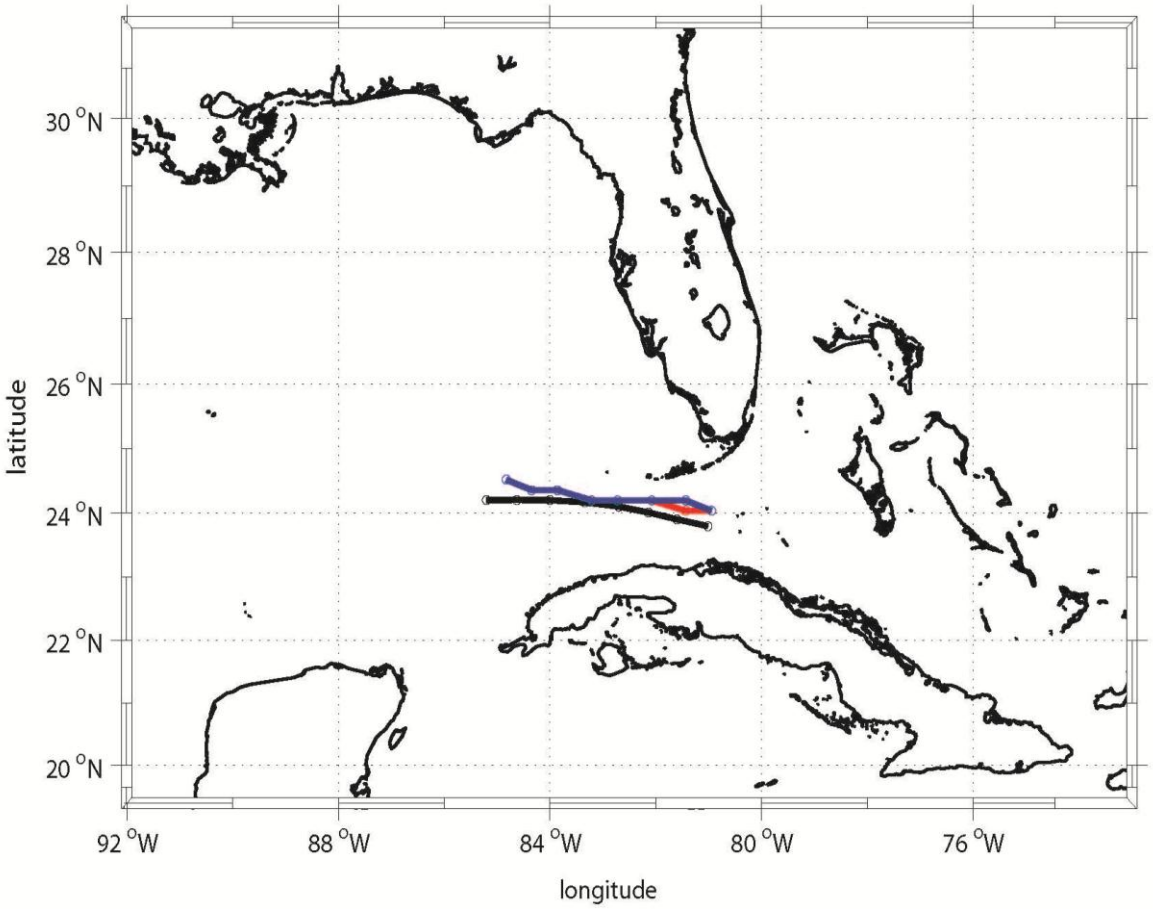

Figure 2. Track forecast for best track data in black, CTL experiment in red, and the CH3 experiment in blue. The data is plotted at 3 hour intervals from September 20 15Z-September 21 12Z.

Overall, the CH3 experiment produced a track forecast that compares well to the CTL. The only exception is at the second time, where the CTL position compares better to the best track. It is interesting to note, however, that the CH3 converges to the best track position at 0Z SEP 21, which was not accomplished by the CH4. Although the CTL outperforms the CH3 experiment in the track forecast, the TC track positions given by the CH3 still present

improvement over the CH4. The track error for CH3 is given by 29. 49 km while the error for CH4 is 29.38 km.

b) *TC Intensity Forecast*

Next, we proceeded to analyze the performance of the CH4 and CTL experiment in the forecast of Hurricane Rita's Intensity. The maximum wind (knots) forecast produced by the CH4 and CTL experiments were compared to the maximum wind values given by the best track. The best track maximum wind values were interpolated with splines at 3 hour intervals, as was done for the TC track, so the times would match those of the CTL and CH4. The results of the maximum wind forecasts are shown in figure 3 with the best track in black, CH4 experiment in blue, and CTL in red.

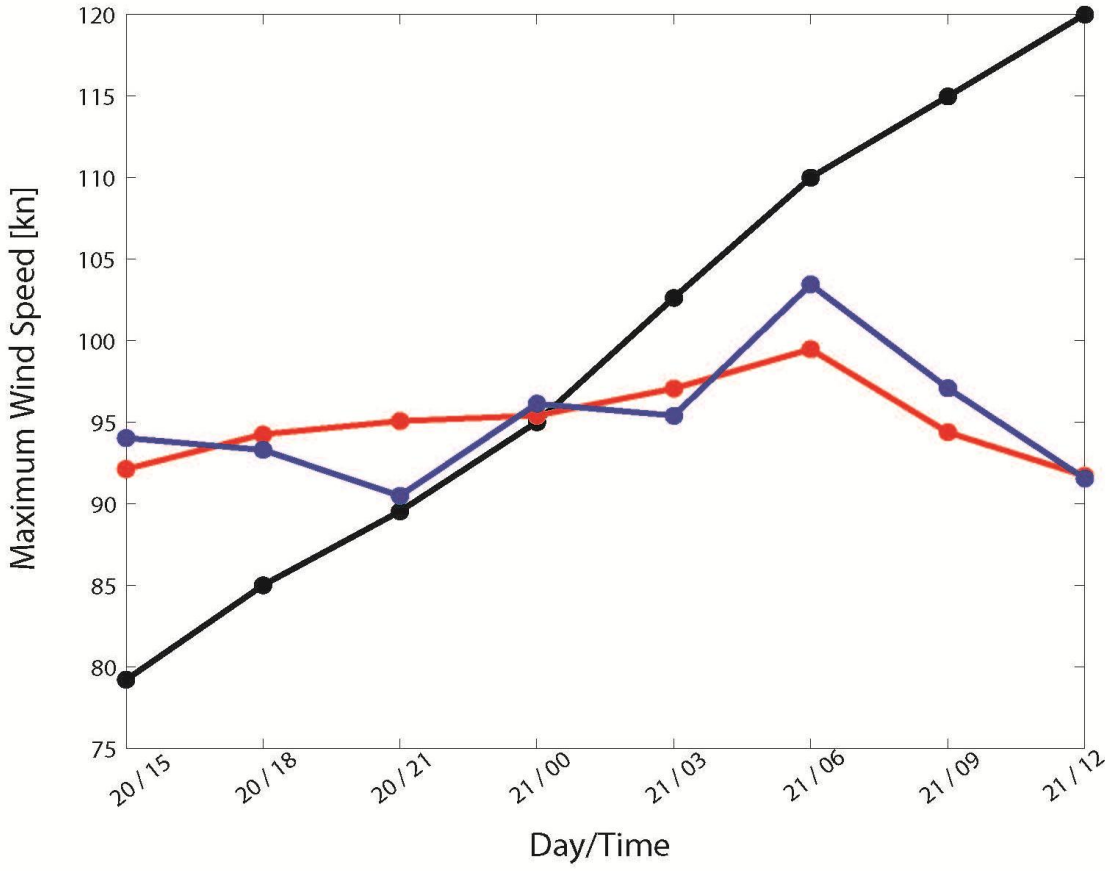

Figure 3. Maximum wind speed forecast in knots (kn) for 15Z SEP 20-12Z SEP 21. The best track data is shown in black, CTL experiment in red, and the CH4 experiment in blue

From the results it is evident that there are very large discrepancies between the best track and the two experiments. At the initial time, both the CH4 and CTL experiments show very high maximum wind values. The initial CH4 maximum wind values are overestimated by approximately 14 knots while the CTL overestimates the maximum wind values by 12 knots. The opposite happens at the final time. At the final time, both the CTL and CH4 converge towards the same value of approximately 92 knots but they fall significantly below the best track, which indicates maximum wind speeds of 120 knots.

Although this was a higher resolution experiment than the one performed in Chapter 2, there are a few reasons that could explain the lack of improvement shown in the results. TC intensity was not assimilated in these experiments, which affects the results. In addition to that, the intensity is taken from the ensemble mean. This will give a greater underestimate or overestimate than taking the mean of the intensities of the individual members. However, it is important to note that although there are overall large discrepancies between the forecasted and best track maximum wind values, there are two times where the CH4 shows similar values to the best track. This occurs at 21Z SEP 20 and 00Z SEP 21. However, the CTL still outperforms the CH4 in this simulation with a root mean square error (RMSE) of 7.92 knots compared to a RMSE of 10.18 knots for the CH4.

The maximum wind speed values for the CH3 experiment were also compared to the CTL and best track estimates for the same time period. The results are shown below in Figure 4 with the best track in black, CH3 in blue, and CTL in red.

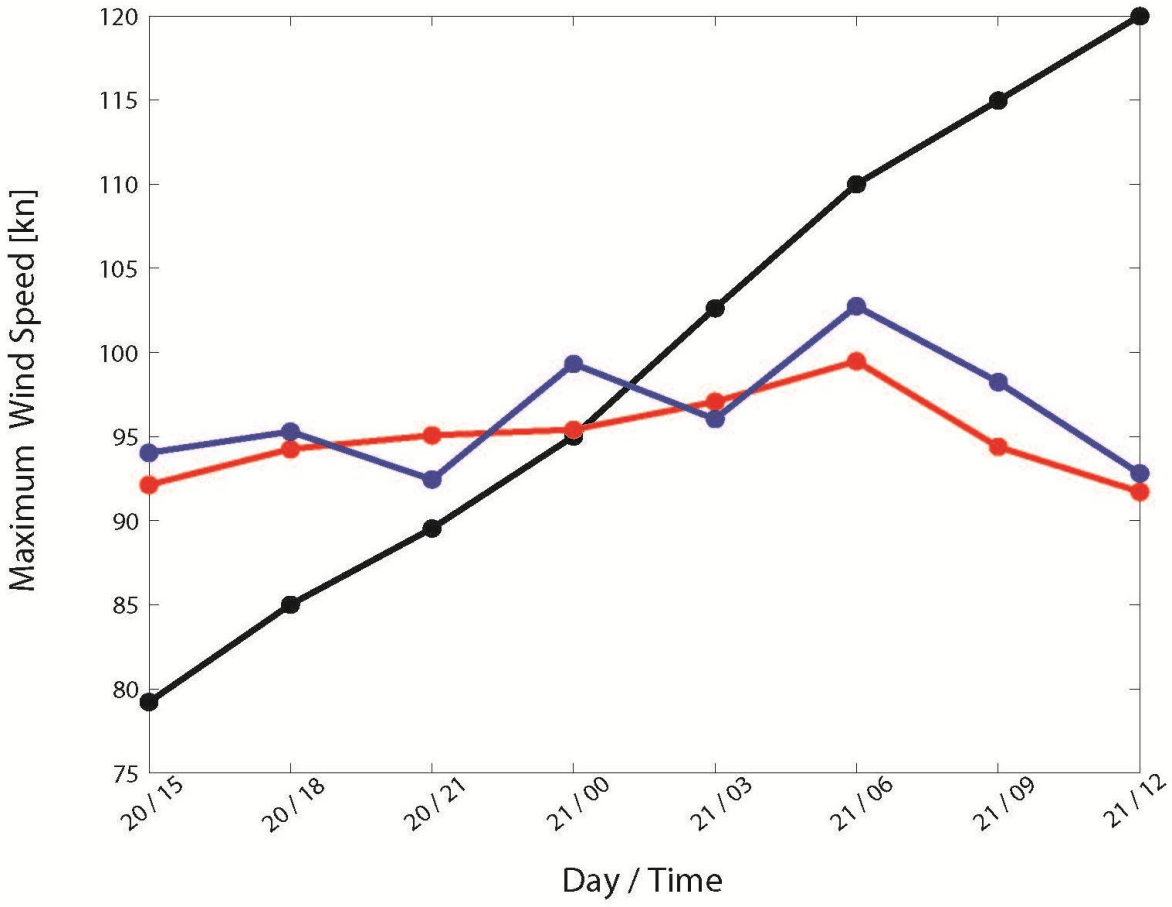

Figure 4. Maximum wind speed forecast in knots (kn) for 15Z SEP 20-12Z SEP 21. The best track data is in black, CTL experiment in red, and the CH3 experiment in blue.

The same issues that both the CTL and CH4 showed in estimating maximum wind speeds are presented by the CH3 experiment. During the first few times the maximum wind speeds are significantly overestimated and at the final times the results fall significantly below the best track. CH3 does not converge towards the wind speeds given by the best track at any of the times while the CTL converges towards the best track value at 00Z SEP 21.

Although the CTL has lower errors than the CH3, the CH3 presents improvement over the CH4 with a RMSE of 9.46 kn compared to 10.18 kn for CH4.

c) *Representation of TC Structure*

After comparing track and intensity errors, observation and simulation results for the CH4 experiment were compared at the beginning, middle and end of the assimilation window in order to assess the overall impact of the assimilation of brightness temperatures in the representation of the TC structure. Figure 5 shows the CTL, CH4 experiment simulation, and observation results, in columns 1, 2 and 3 respectively. The data is plotted for three different times: 15Z SEP 20 in row 1, 03Z SEP 21 in row 2, and 12Z SEP 21 in row 3.

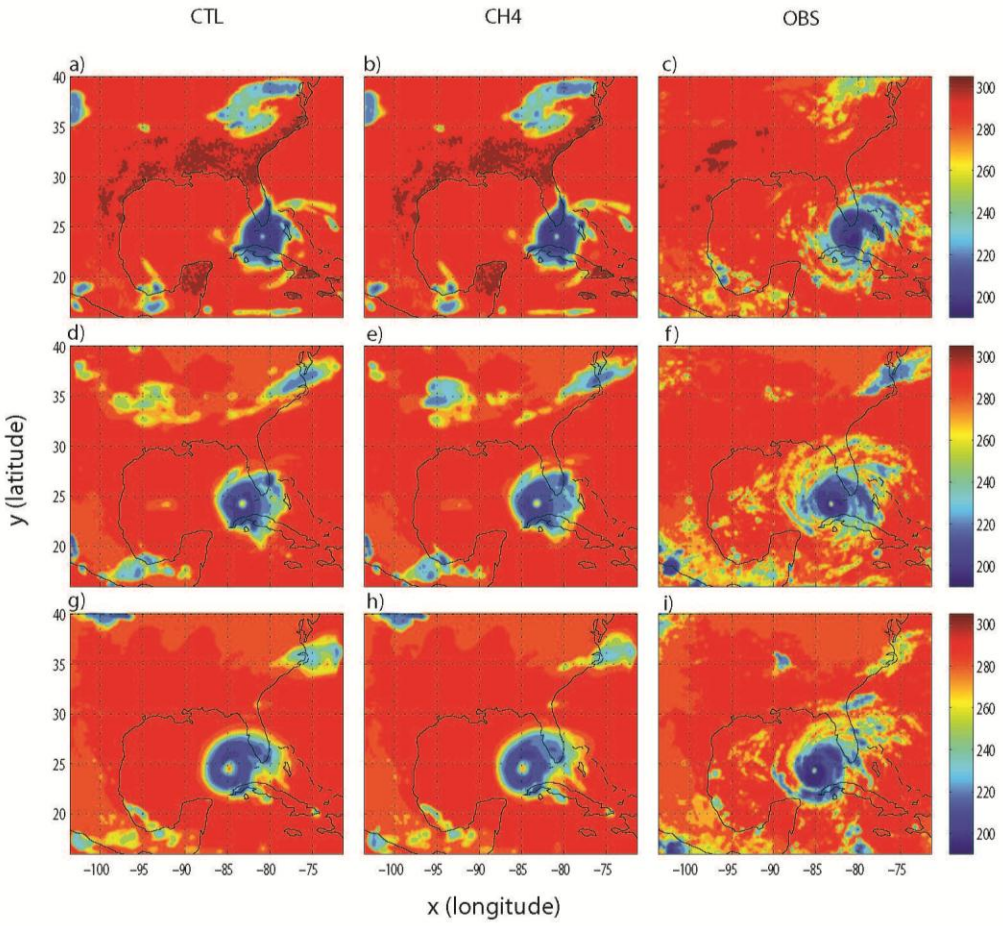

Figure 5. CTL, simulation, and observation results of GOES Channel 4 T_B (˚K) at the beginning, middle, and end of the assimilation window. GOES Channel 4 CTL data is plotted in column 1, simulation results are plotted in column 2, and observations are plotted in column 3. The data is plotted for 15Z September 20 (row 1), 03Z September 21 (row 2), and 12Z September 21 (row 3).

Overall, the TC structure shown in the CTL and CH4 figures is very similar. There are only a few differences that can be noticed. For the second time, the CTL shows that the TC extends further south below Cuba than in shown in CH4. At the final time, however, the size of the TC shown by CH4 is much larger than the CTL. Other than this, brightness temperature values for both experiments are overall the same in the all regions of the storm.

There are a few differences that are more evident when comparing the results given by the observations (panel 3) with the CTL and CH4 results. The eye of the storm in the observations is much smaller than the one produced by CH4 and CTL. The rain bands also cover a larger area in the observations than in the CTL and CH4. There is a small low pressure region in the Pacific (near Mexico) that was produced by the observations. Although the CH4 and CTL also produced this feature, it is not an intense as shown by the observations. However, the CH4 and CTL brightness temperature values in the region of the TC compare well to those produced by the observations.

The same analysis of TC structure that was performed for the CH4 observations was also done for CH3. Observation and simulation results for the CH3 experiment were compared for the same time periods to assess the overall impact of the assimilation of brightness temperatures in the representation of the TC structure. The results are shown in Figure 6 below. The CTL, CH3 experiment simulation, and observation results are shown in columns 1, 2 and 3 respectively. The data is plotted for 15Z SEP 20 in row 1, 03Z SEP 21 in row 2, and 12Z SEP 21 in row 3.

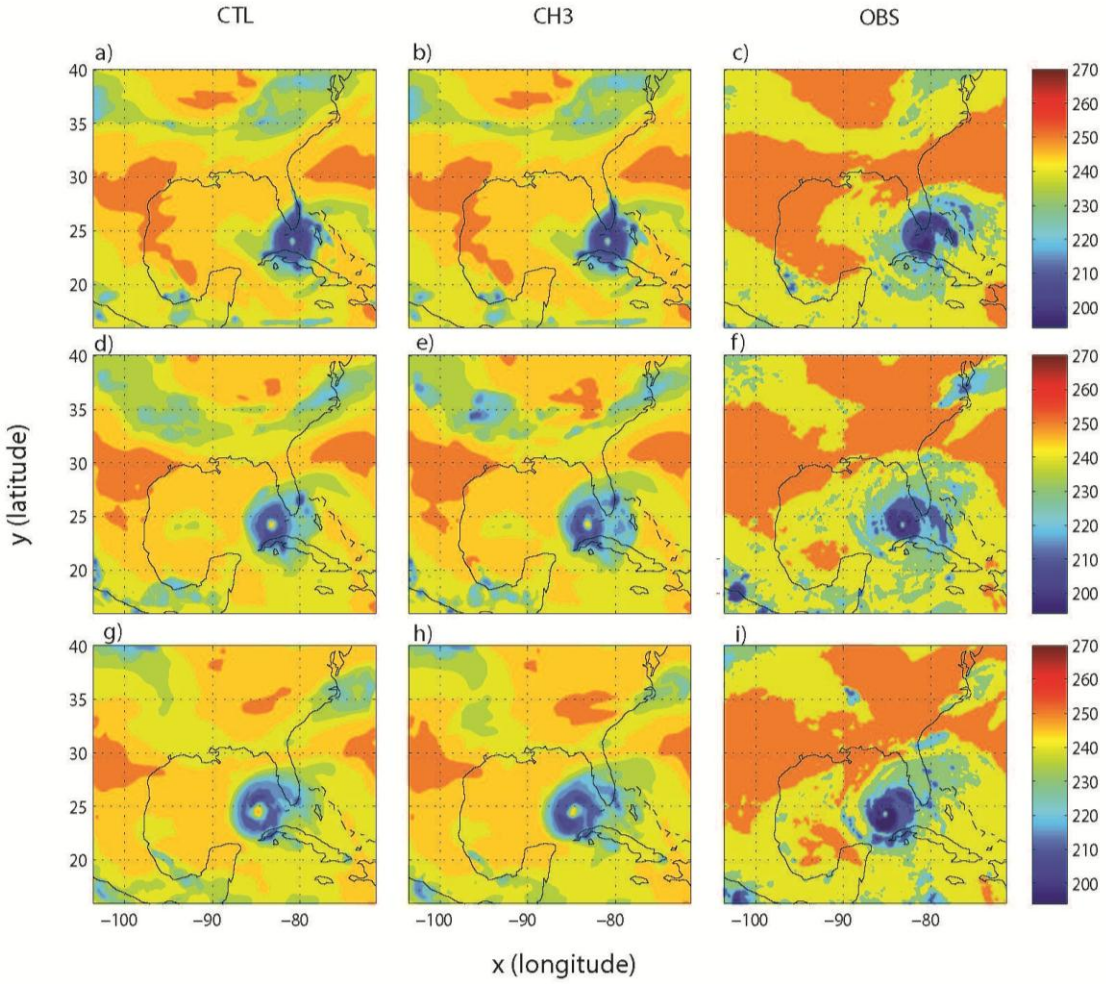

Figure 6. CTL, observation, and simulation results of GOES Channel 3 T_B (˚K) at the beginning, middle, and end of the assimilation window. GOES Channel 3 CTL data is plotted in column 1, simulation results are plotted in column 2, and observations are plotted in column 3. The data is plotted for 15Z September 20 (row 1), 03Z September 21 (row 2), and 12Z September 21 (row 3).

There weren't many marked differences between the CTL and CH3 results in the representation of TC structure. The only evident difference is the storm radius, which is a bit lager for the CH3 experiment, especially at the end of the assimilation window. Other than

the storm radius, both experiments produced the same features in the same locations and brightness temperature values are overall the same.

However, there are significant differences when comparing the CH3 and CTL results to the observations. First, the storm radius (eye) is much larger (smaller) in the observations than in the CH3 and CTL. In addition to this, the low pressure region shown by the observations is not as intense in the CH3 and CTL. This was also the case with the CH4 observations. The most evident difference, however, is in the storm intensity. The storm produced by the CH3 and CTL is much weaker than the one produced by the observations. Brightness temperature values produced by the observations are significantly lower than those shown by CH3 and CTL, especially in the region closest to the TC core.

d) *Microphysical Fields*

A few different variables were selected to examine the performance of the CH4 experiment relative to the CTL in the representation of these fields. The selected fields are u wind component, v wind component, and sea level pressure. A microphysical field, precipitable water, as also selected to determine if the relationship between microphysics and brightness temperatures leads to an improved representation of the field. The differences between the CTL and CH4 experiment are examined by subtracting the CTL from the CH4 results and plotting these differences. The results are shown in Figure 7.

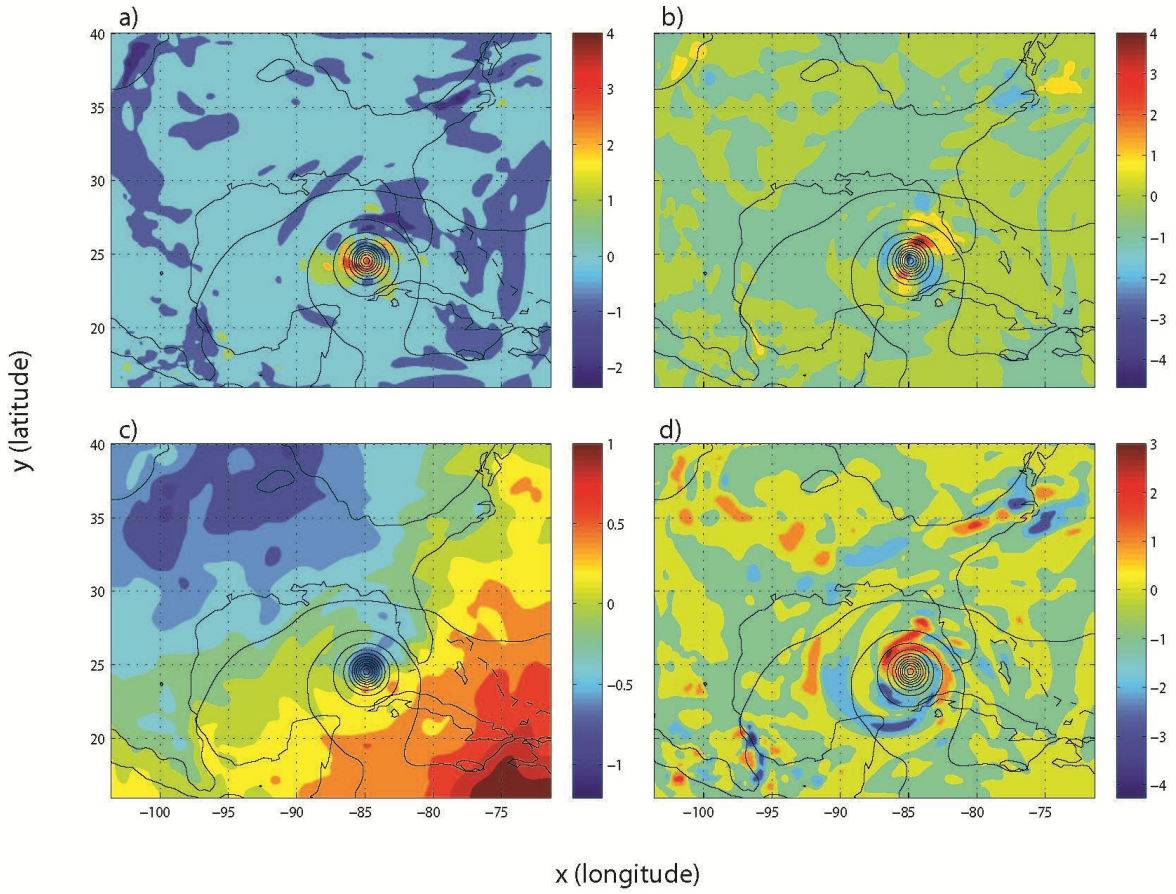

Figure 7. CTL and CH4 differences for u wind component at 1176m height (a), v wind component at 1176m height (b), SLP (c), and Precipitable Water (d). SLP for the CTL experiment was contoured over each field from 970-1030m at 5m intervals

From the results it is evident that there are significant differences between the CH4 and CTL results for all the selected fields. The u wind component, v wind component, and precipitable water show the largest differences. Both experiments show disagreements in different portions of the storm center. Since the ensemble members are created via

perturbations of the TC vortex, any differences in the vortex position, regardless of how small, will lead to significant differences in the results.

In the case of the SLP field, the maximum difference between the CTL and CH4 results is of approximately 1.5 hPa and occurs in the TC center. The CH4 experiment produced lower SLP values than the CTL in the TC core. Although the CH4 SLP values were overall lower than those of the CTL, and lower SLP values are correlated to a weaker storm, it still was not sufficient to produce an accurate forecast of maximum winds for the initial times where the storm was still weak, as was shown in Figure 3.

The representation of the selected variables by the CH3 experiment was also examined. The differences between the CTL and CH3 experiment were examined by subtracting the CTL from the CH3 results and plotting these differences. The results are shown in Figure 8.

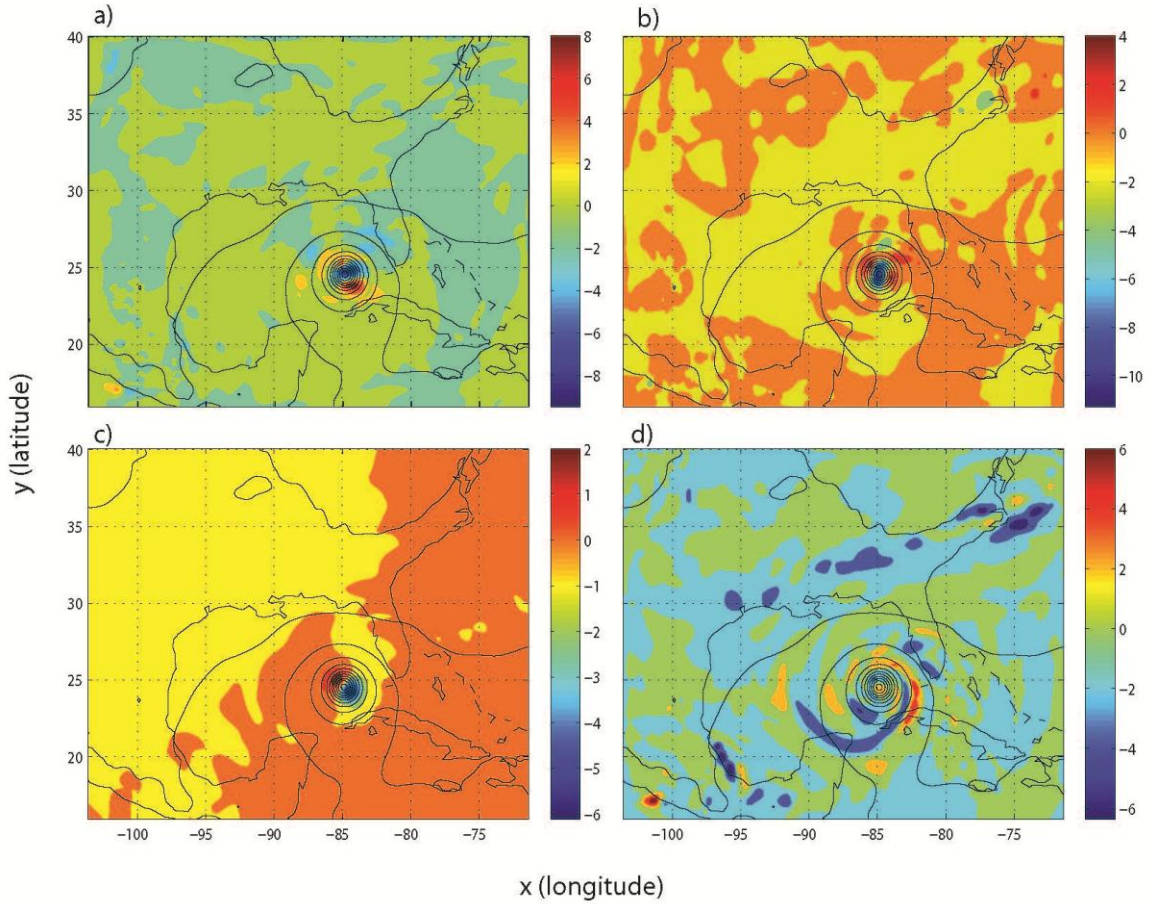

Figure 8. CTL and CH3 differences for u wind component at 1176m height (a), v wind component at 1176m height (b), SLP (c), and Precipitable Water (d). SLP for the CTL experiment was contoured over each field from 970-1030m at 5m intervals

Overall, the differences between the CTL and CH3 results are larger and are mostly confined to the eye and a portion of the inner eye wall of the TC. The only exception is in the precipitable water field, where the discrepancies between the CH3 and CTL extend significantly past the inner eye wall. However, the differences between the CH4 and CTL are still smaller in all the cases.

e) *Non-Microphysical Fields*

As a final analysis, the root mean square (RMS) error of the ensemble mean for 14 different observed fields was examined to quantitatively assess the overall impact of the assimilation of GOES CH4 T_B on the forecast of each field. The RMS error (RMSE) indicates the forecast error and was calculated using equation (4) on Chapter 2. The errors were calculated as the average RMS errors over all times for each field. The RMSE results are summarized in the left side panel of Table 1.

Observation Type	**Experiments**			
	RMS Errors		**Calibration**	
	CTL	CH4	CTL	CH4
Max Wind (kn)	7.9163	10.1829	1.0179	1.3737
AMV u (m/s)	3.6772	3.7023	.7965	.7952
AMV v (m/s)	3.3111	3.3154	.7120	.7119
SLP (hPa)	1.3230	1.3673	.8171	.8445
RAOB U (m/s)	2.8465	2.8197	.7910	.7708
RAOB V (m/s)	2.7331	2.7569	.7629	.7593
RAOB Z (m/s)	10.6690	10.2128	.4318	.4073
RAOB T (K)	1.0688	1.0589	.6598	.6564
CH3 T_B (K)	5.1392	3.8410	.9793	.9358
CH4 T_B (K)	6.3151	6.0438	.3884	.3787
ACARS U (m/s)	3.2543	3.2744	.8627	.8675
ACARS V (m/s)	3.0690	3.1053	.8157	.8233
ACARS T (K)	1.4180	1.4244	1.0328	1.0363
Vortex Latitude	.1878	.2175	1.4311	1.5963
Vortex Longitude	.1355	.1336	.9438	.8769

Table 1. RMS errors and calibration values for the CTL and CH4 experiment averaged over the eight assimilation cycles for each field. Errors for max wind, AMV u, AMV v, RAOB U, RAOB V, RAOB Z, ACARS U, and ACARS V are in m/s. Errors for SLP are in hPa. Errors for ACARS T, RAOB T, CH3 $\boldsymbol{T_B}$, and CH4 $\boldsymbol{T_B}$ are in K.

Overall, the RMS errors show that there was little improvement produced by the assimilation of GOES CH4 brightness temperatures. The RMS errors for the CTL are lower than the CH4 for most of the fields. The only fields where the CH4 outperformed the CTL were RAOB U, RAOB T, RAOB Z, vortex longitude, CH3, and CH4. Interestingly, the field where the CH4 presented the most improvement over the CTL was for CH3 water vapor.

The RMS errors for all the fields were also examined for the CH3 experiment. Results are shown below in the left panel of Table 2.

Observation Type	**Experiments**			
	RMS Errors		**Calibration**	
	CTL	CH3	CTL	CH3
Max Wind (kn)	7.9163	9.4553	1.0179	1.1441
AMV u (m/s)	3.6772	3.6184	.7965	.7884
AMV v (m/s)	3.3111	3.3151	.7120	.7144
SLP (hPa)	1.3230	1.3375	.8171	.8276
RAOB U (m/s)	2.8465	2.6904	.7910	.7805
RAOB V (m/s)	2.7331	2.8284	.7629	.7832
RAOB Z (m/s)	10.6690	10.5203	.4318	.4077
RAOB T (K)	1.0688	1.0624	.6598	.6634
CH3 T_B (K)	5.1392	3.6014	.9793	.9026
CH4 T_B (K)	6.3151	5.8298	.3884	.3757
ACARS U (m/s)	3.2543	3.3070	.8627	.8760
ACARS V (m/s)	3.0690	3.1132	.8157	.8263
ACARS T (K)	1.4180	1.4215	1.0328	1.0353
Vortex Latitude	.1878	.1910	1.4311	1.4157

Vortex Longitude	.1355	.1601	.9438	1.0547

Table 2. RMS errors and calibration values for the CTL and CH3 experiment averaged over the eight assimilation cycles for each field. Errors for max wind, AMV u, AMV v, RAOB U, RAOB V, RAOB Z, ACARS U, and ACARS V are in m/s. Errors for SLP are in hPa. Errors for ACARS T, RAOB T, CH3 $\boldsymbol{T_B}$, and CH4 $\boldsymbol{T_B}$ are in K.

Although the errors of the CTL experiment are still lower than those of the CH3, the CH3 RMS errors are overall lower than the CH4s for 7 different fields. Also, the CH3 presents marked improvement over the CTL in CH4 brightness temperatures, CH3 water vapor, RAOB T, RAOB Z, RAOB U, and AMV u. The most significant improvement was in the CH3 water vapor field.

In addition to RMS errors, calibration values were calculated to further assess the impact of the assimilation on the results. The calibration is defined as the square of the innovation divided by the square of the ensemble spread. The innovation and ensemble spread are defined by equation (6) and (7) on Chapter 2. Calibration values were calculated as the average calibration over all times for each field. The calibration results for the CH4 and CTL experiments are found on the right side panel of Table 1 and those for the CH3 are found on the right hand panel of Table 2.

According to the calibration values, the CH4 performed better than the CTL in the ACARS U, ACARS V, and SLP cases. The AMV u and AMV v results also compare well to the CTL, even though the CTL results were better. In the CH3 case, the AMV v, SLP, RAOB V, RAOB T, ACARS U, ACARS V and Vortex Latitude present marked improvement over the CTL. Vortex longitude is the case where the CTL significantly outperforms the CH3.

Upon analysis of the calibrations, the CH3 presents significant improvement over the CH4. The CTL, however, presents overall the most improved results.

4.4) Conclusions

An EnKF data assimilation scheme incorporating a bogus vortex TC initialization method was employed to simulate Hurricane Rita for the time period of 15Z SEP 20 to 12Z SEP 21. Three experiments were performed to determine if assimilating GOES-12 observations along with conventional observations would produce an improvement in TC forecasts and representation of vortex structure over experiments incorporating conventional observations only. The CH4 experiment incorporated conventional observations and GOES-12 brightness temperatures, the CH3 experiment incorporated conventional observations and GOES-12 water vapor observations, and the final CTL experiment incorporated conventional observations only.

Overall, results from the experiments showed that the assimilation of GOES-12 brightness temperatures and water vapor observations produce limited improvement in all fields that were examined when compared to the experiment that incorporated conventional observations only (CTL). In the track forecast, average track errors for the CH4 and CH3 experiments exceeded the CTL errors by 2.81 km and 2.92 km respectively. For intensity and all other fields that were examined, RMS errors for CH3 and CH4 were also above CTL errors for most cases. There are a few exceptions, however, where RMS errors for CH3 and

CH4 are lower than those for the CTL. Based on RMS errors, the CH4 experiment performed better than the CTL in RAOB (U, Z, T), vortex longitude, and CH3 and CH4 brightness temperatures. The CH3 experiment, on the other hand, performed better than the CTL in RAOB (U, Z, T), AMV (u), as well as CH3 and CH4 brightness temperatures. For the most part, CH3 and CH4 produced improved results over the CTL in the representation of the same variables.

Although the CTL produced overall the best results, assimilating GOES-12 water vapor observations produced more improvement than assimilating GOES-12 brightness temperature observations in most cases that were examined. CH4 performed better than CH3 in the track forecast. However, CH3 outperformed CH4 in the intensity forecast with an RMS error of 9.45 kn compared to 10.18 kn for CH4. RMS errors for the rest of examined fields are also overall lower for CH3. CH3 produced RMS errors lower than CH4 for 10 of the different fields examined in Table 1 and 2. CH3 observations are expected to produce more improvement than CH4 observations as the "water vapor" channel generally contains information about the middle and upper-troposphere in clear-sky conditions, and about the cloud-tops in cloudy conditions. CH4, on the other hand, can only see the surface in clear-sky conditions.

There are certain things that can be improved upon for better assimilation results. An alternate approach that could be employed to create an ensemble of analyses is to perturb both the environment and the TC vortex. This would allow quantification of the ensemble spread in both the environmental flow and TC vortex. Without spread in the environment,

observations can only impact the vortex itself. While perturbing only the TC vortex allows decoupling of the environmental-scale and vortex-scale impacts, it also has the effect of not allowing any communication between the vortex and the environment and the observations. In reality, the interaction between the environment and TC vortex is a highly complicated feedback process. Therefore, perturbing both the environment and vortex structure would be a way to account for the environment's impact on the TC (and vice versa).

Despite the results obtained in this study, the assimilation of GOES-12 infrared data shows potential for application in assimilation schemes with an EnKF for TC forecasting. Results from the experiments performed in Chapter 2 clearly support this hypothesis. RMS errors for certain fields that were examined in this Chapter also show that GOES observations show potential for TC intensity forecasting. Modifications in methodology, however, are necessary to optimize the performance of this scheme and use the GOES-12 information efficiently. Work is already being done to improve upon the methodology described in this study. Further research should be done to continue exploring the potential of the assimilation of radiance data from the different channels on GOES-12 as the temporal and spatial continuity of these observations can be an invaluable asset for TC forecasting.

References

Bender, M. A., I. Ginis, R. Tuleya, B. Thomas, and T. Marchok, 2007: The operational GFDL coupled hurricane–ocean prediction system and a summary of its performance. Mon. Wea. Rev., 135, 3965–3989.

Houtekamer, P.L., and H. L. Mitchell, 2001: A Sequential Ensemble Kalman Filter for Atmospheric Data Assimilation. *Mon*. *Wea*. *Rev*., **129**, 123–137.

Iwasaki, T., Nakano, H., and M. Sugi, 1987: The performance of a typhoon track prediction model with convective parameterization. J. Meteor. Soc. Japan, 65, 555–570.

Koyama, T., Vukicevic, T., Sengupta, M., Haar, T. V., and A. S. Jones, 2006: Analysis of Information Content of Infrared Sounding Radiances in Cloudy Conditions. *Mon*. *Wea*. *Rev*., **134**, 3657–3667.

Kurihara, Y., M. A. Bender, and R. J. Ross, 1993: An initialization scheme of hurricane models by vortex specification. Mon. Wea. Rev., 121, 2030–2045.

Kurihara, Y., M. A. Bender , R. E. Tuleya, and R. J. Ross, 1995: Improvements in the GFDL hurricane prediction system. Mon. Wea. Rev., 123, 2791–2801.

Kwon, In-Hyuk, Hyeong-Bin Cheong, 2010: Tropical Cyclone Initialization with a Spherical High-Order Filter and an Idealized Three-Dimensional Bogus Vortex. *Mon*. *Wea*. *Rev*., **138**, 1344–1367

Leslie, L. M., and G. J. Holland, 1995: On the bogussing of tropical cyclones in numerical models: A comparison of vortex profiles. Meteor. Atmos. Phys., 56, 101–110.

Pu, Z. X., and S. A. Braun, 2001: Evaluation of bogus vortex techniques with four-dimensional variational data assimilation. Mon. Wea. Rev., 129, 2023–2039.

Rogers, R., and Coauthors, 2006: The Intensity Forecasting Experiment: A NOAA Multiyear Field Program for Improving Tropical Cyclone Intensity Forecasts. *Bull*. *Amer*. *Meteor*. *Soc*., **87**, 1523–1537.

Serrano, E., and P. Unde´ n, 1994: Evaluation of a tropical cyclone bogussing method in data assimilation and forecasting. Mon. Wea. Rev., 122, 1523–1547.

Thu, T. V., and T. N. Krishnamurti, 1992: Vortex initialization for typhoon track prediction. Meteor. Atmos. Phys., 47, 117–126.

Wang, D., X. Liang, Y. Zhao, and B. Wang, 2008: A comparison of two tropical cyclone bogussing schemes. Wea. Forecasting, 23, 194–204.

Zhang, X., Q. Xiao, and P. J. Fitzpatrick, 2007: The impact of multisatellite data on the

initialization and simulation of Hurricane Lili's (2002) rapid weakening phase. Mon. Wea. Rev., 135, 526–548.

Zou, X., and Q. Xiao, 2000: Studies on the initialization and simulation of a mature hurricane using a variational bogus data assimilation scheme. J. Atmos. Sci., 57, 836–860.

Chapter 5

Conclusions

5.1) Summary and Future Work

This thesis study explored the potential of GOES-12 10.7 micron brightness temperatures and 6.5 micron water vapor observations for use in an EnKF scheme to improve forecasting and predictability of tropical cyclones. Two studies were performed to determine if assimilation of GOES-12 observations in conjunction with conventional observations would lead to improved results over a scheme that assimilates conventional observations only. The impact of assimilating GOES-12 observations was examined via analysis of TC track & intensity forecasts, TC structure representation, and representation of microphysical and non-microphysical fields.

In the first study (Chapter 2), GOES-12 10.7 micron brightness temperatures were assimilated with an EnKF scheme where ensemble members created via perturbations of the environment. The results obtained from this coarse resolution experiment showed that the assimilation of GOES-12 channel 4 brightness temperatures with an EnKF produces track and intensity errors lower than simulations that involve conventional observations only. The temporal continuity of GOES data produces a more realistic TC structure at the initial time. Such improved representation at the initial time allows the simulation to generate more accurate track and intensity forecasts. In addition to this, the assimilation of GOES-12 brightness temperatures produced an improved representation of microphysical and non-

microphysical fields. The SLP field showed evidence of the improvement in the representation of non-microphysical fields since the assimilation of GOES T_B eliminated the spurious cyclone that developed in the CTL experiment. Therefore, in addition to producing more accurate track and intensity forecasts, assimilation of GOES T_B shows promise in eliminating the existing numerical weather prediction issues with spurious cyclone genesis.

In the second set of experiments performed in this thesis study (Chapter 4), GOES-12 brightness temperatures and water vapor observations were both assimilated with an EnKF. The goal in this study was to determine which set of observations (assimilated in conjunction with conventional observations) would produce more improved results over the CTL experiment. Different from the experiments in Chapter 2, a higher resolution of 18km was employed as well as a bogussing scheme for TC initialization. In addition to this, ensemble members were created via perturbations of the TC vortex.

An additional difference to note between the experiments in Chapter 2 and Chapter 4 is that the CH3 and CH4 satellite observations in Chapter 4 were bias corrected. NWP models are not perfect and therefore, have systematic biases that may make the model state drift towards the model climatology. This generates simulated observations that significantly differ from the real world climatology (Delworth et al., 2005;Collins et al., 2006), that is, observations that are biased. Bias correction can then be employed to correct this bias. It minimizes the error of the next forecast using bias from past errors. Bias correction is extremely important as forcing the model towards the observations would affect the model

prognostic variables. In the case of brightness temperatures, temperature, mixing ratio and vertical velocity would be impacted.

Overall, results from the experiments showed that the assimilation of GOES-12 brightness temperatures and water vapor observations produce limited improvement when compared to the experiment that incorporated conventional observations only (CTL). Average track and RMS errors were significantly higher for the experiments that assimilated GOES-12 brightness temperatures and water vapor observations. However, there were a few exceptions where RMS errors for CH3 and CH4 were lower than those for the CTL. This was the case for RAOB (U, Z, T), and CH3 and CH4 brightness temperatures variables.

Although the experiment assimilating conventional observations produced overall the best results, assimilating GOES-12 water vapor observations produced more improvement than assimilating GOES-12 brightness temperature observations in most cases that were examined. CH4 may have performed better than CH3 in the track forecast, but CH3 outperformed CH4 in the intensity forecast with an RMS error of 9.45 kn compared to 10.18 kn for CH4. RMS errors for the rest of examined fields were also overall lower for CH3.

Given the mixed results that were obtained from both studies, more experimentation is required in order to reach more conclusive results. There are certain modifications that can be made to this scheme that may aid in improving assimilation results. Covariance localization is often applied in studies to improve upon assimilation results and eliminate spurious correlations (Campbell and Bishop, 2009). While horizontal covariance localization was applied in this study, vertical covariance localization may have further aided

in improving results. Current covariance models are stationary and assume uniformity in the vertical, which is not necessarily true for observations near the surface. Thus, the performance of stationary covariance models can be limited if observations near the surface are incorporated. For this reason, vertical localization may be crucial to obtain more accurate results when the ensemble assimilation involves the use of surface data (Hacker et. al. 2007). This could prove to be especially beneficial in the assimilation of intensity.

A second modification that can be made to our scheme is to use perturbations of both the environmental flow and the TC vortex to create the ensemble members. The ensemble members in the first set of experiments ensemble members were created via perturbations of the environmental flow while in the second set of experiments they were created via perturbations of the TC vortex. Employing a method that combines both methods could lead to significant improvement as the uncertainty associated with both sources (environmental flow and TC vortex) will be included in the analyses of ensemble members. While TC track is mostly driven by environmental steering, TC intensity could benefit from accounting the uncertainty associated with both sources.

Finally, more case studies are necessary to further assess the impact of incorporating GOES-12 observations for TC forecasting. This single case study proved that there is potential in this scheme. However, all storms are different and there are countless scenarios that could lead to significantly different results. With a larger sample of TCs it would be possible to reach more definitive conclusions on the impact of this scheme.

In conclusion, although the second set of experiments was not as successful as the first, the assimilation of GOES-12 radiance data still shows potential for improving forecasts

and predictability of tropical cyclones. GOES-12 data provides the temporal and spatial continuity that can be an asset for improving representation of TCs in the model initial conditions. GOES provides continuous over the region of tropical cyclone genesis and development. More importantly, GOES provides continuous observations of the TC core region, which is not viable with any other existing data collection methods. Observations over the TC core region are crucial for TC intensity forecasting and also to fill gaps in the current understanding of TC intensification dynamics. Modifications must be made to the experiments to further optimize the use of these observations as this was only an exploratory study. Further research should be done to explore the potential of GOES-12 brightness temperatures and water vapor observations as well as other observations from the different channels on GOES.

References

Campbell, W. F., Bishop, C. H, and D. Hodyss, 2010: Vertical Covariance Localization for Satellite Radiances in Ensemble Kalman Filters. *Mon*. *Wea*. *Rev*., **138**, 282–290.

Collins, W. D., Bitz, C. M., Blackmon, M. L., Bonan, G. B., Bretherton, C. S. and co-authors, 2006: The Community Climate System Model Version 3 (CCSM3). *J*. *Clim*., **19**, 2122-2143.

Delworth, T. L., Broccoli, A. J., Rosati, A., Balaji, R. J. S. V., Beesley, J. A. and co-authors. 2005. GFDL's CM2 global coupled climate models, Part I: Formulation and

simulation characteristics. *J*. *Clim*., **19(5)**, 643-674.

Hacker, J. P., Anderson, J. L., and M. Pagowski, 2007: Improved Vertical Covariance Estimates for Ensemble-Filter Assimilation of Near-Surface Observations. *Mon*. *Wea*. *Rev*., **135**, 1021–1036.

Approved:_____

Gregory J. Tripoli

Professor, Department of Atmospheric and Oceanic Sciences

Date:_____

Approved:_____

William E. Lewis

Research Advisor, Space Science and Engineering Center

Date:_____